Molecular Characterization of Phosphorous Starvation Tolerance 1 Gene in Wheat

Thesis submitted in the partial fulfilment of requirements for the degree of

MASTER OF PHILOSOPHY

IN

PLANT GENOMICS AND BIOTECHNOLOGY

BY

HINA ABBAS

Department of Plant Genomics and Biotechnology

PARC Institute of Advanced Studies in Agriculture

National Agricultural Research Center, Islamabad

Quaid-I-Azam University Islamabad, Pakistan

2021

Molecular Characterization of Phosphorous Starvation Tolerance 1 Gene in Wheat

A Thesis
Submitted to Quaid-i-Azam University, Islamabad, in the partial fulfillment of the requirements for the degree of

MASTER OF PHILOSOPHY
IN
PLANT GENOMICS AND BIOTECHNOLOGY

By

Hina Abbas

Department of Plant Genomics and Biotechnology
PARC Institute of Advanced Studies in Agriculture
National Agricultural Research Centre, Islamabad
Quaid-I-Azam University, Islamabad, Pakistan

2021

Dedication

I dedicate my humble attempt and all of the hard work

to my loving and caring parents,

Ghulam abbas and Tanveer Kousar,

Their love, encouragement, and efforts

made me the person I am today

Most of all, this work is dedicated to my brother

Ali Abbas

without his support and efforts,

I would never have made it this far

Thank you all

For always being there

AUTHOR'S DECLARATION

I, **Hina Abbas,** hereby declare that the data presented in this thesis, " **Molecular Characterization of Phosphorous Starvation Tolerance 1 Gene in Wheat** " is generated by me from original research work during the scheduled period of study under the supervision of **Dr. Muhammad Ramzan Khan**. The results and materials used in this thesis were never presented anywhere else earlier.

Date: _____

Hina Abbas
Reg # 02361913007

PLAGIARISM REPORT

It is certified that **Miss Hina Abbas** (02361913007) has submitted her M. Phil thesis titled " **Molecular Characterization of Phosphorous Starvation Tolerance 1 Gene in Wheat** " that has been checked on Turnitin for similarity index (plagiarism).

Overall plagiarism = 8% that lies in the limit provided by HEC (19%)

Dr. Muhammad Ramzan Khan
Principal Scientific Officer
NIGAB, NARC, Islamabad

TABLE OF CONTENTS

LIST OF FIGURES

LIST OF TABLES

LIST OF ABBREVIATIONS

Word	Abbreviation
CWANA	Central West Asia and North Africa
CIMMYT	International Maize and Wheat Improvement Centre
ICARDA	International Centre for Agriculture Research in the Dry Areas
PUE	Phosphorus Use Efficiency
PSR genes	Phosphate starvation responsive genes
RCA	Root cortical aerenchyma
PAPs	Purple Acid Phosphatases
TaPSTOL1	*Triticum aestivum* Phosphorus Starvation Tolerance 1
BLAST	Basic Local Alignment Search Tool
SMART	Simple Modular Architecture Research Tool
MEME	Motif-Based Sequence Analysis Tools
GSDS	Gene Structure Display Server
IWGSC	The International Wheat Genome Sequencing Consortium
ParaAT	Parallel Alignment and back - Translation
GFF3	General Feature Format
TPM	Transcript per Million
NDVI	Normalized Difference Vegetation Index
TRIzol	Total RNA Isolation
TAE Buffer	Tris-Acetate-EDTA
bps	Base Pairs
Mbs	Mega Base Pairs
MYA	Million Years Ago
cDNA	Complementary Deoxyribonucleic Acid
cm	Centimeter
DNA	Deoxyribonucleic Acid

dNTPs	Deoxynucleotide triphosphates
MEGA	Molecular Evolutionary Genetic Analysis
mg	Milligram
ml	Milliliter
NARC	National Agricultural Research Center
NCBI	National Centre for Biotechnology Information
NIGAB	National Institute for Genomics and Advanced Biotechnology
PCR	Polymerase Chain Reaction
pH	Power of Hydrogen Ion
qRT-PCR	Quantitative Real Time PCR
RNA	Ribonucleic Acid
rpm	Revolutions Per Minute
ul	Microliter
ug	Micro gram
uM	Micro molar

ACKNOWLEDGEMENTS

I am grateful and like to thank **ALMIGHTY ALLAH**, The Most Merciful, the Beneficent, who gave me the courage and support to complete this study and thesis write-up. Cordial gratitude to **PROPHET MUHAMMAD (PBUH),** who is forever a torch of guidance and knowledge for humanity. All facilities, abilities, opportunities, strength, and powers given to me are blessed by ALLAH almighty for this level of study and research in such a vibrant environment

I want to express my sincere gratitude and pay special regards to my honorable supervisor **Dr. Muhammad Ramzan Khan**, Principal Scientific Officer, NIGAB, NARC, Islamabad, for his patience, motivation, continuous support, and efforts to complete the completion of my thesis research work.

I want to express my gratitude to the Director of NIGAB, **Dr. Aish Muhammad**, Principal Scientific Officer, for providing an excellent and work-friendly environment at NIGAB. I would also like to express special gratitude to my co-supervisor, **Dr. M. Kashif Naeem,** for providing me with much assistance and guidance throughout the research period. I thank him with utmost sincerity for his help and all the things he taught me. I want to thank **Ma'am Safeena**, Scientific Officer, NIGAB, and **Dr. Nazia Rehman**, Senior Scientific Officer, NIGAB, for their help and guidance.

I want to thank my colleagues of session 2019-2021 for all the joyous, happy, sad, fun, and academic activities during the whole academic session. I want to thank all my teachers and lab fellows, especially **Aliya Errum**, **Nageen Zahra, Ammar Amanat, Muhammad Umer,** for their kind cooperation, assistance, and help. I want to pay special thanks to my respected senior and good friend **Shehla Shoukat** for all the assistance, guidance, help, and fun times that helped me in research and hostel life.

I want to express my most special gratitude to my friends **Fabia Fakhar Zaman, Maryam Mubeen, Sehrish Bashir, Marya Rubab, Uswa Ikram, and Farwa Tallat.** The hostel life would have been too boring and lonely without their presence. The research and all the work would have been too tiresome, laborious, and lifeless. I will dearly miss all the happy and sad moments we shared.

I would also like to express my deepest gratitude to my friends, **Javeria Jehangir, Abbiha Tahir Kazmi,** and **Sharukh Ihsan,** for always being there whenever I felt down and needed a push.

In the end, I am incredibly grateful to my **Parents, Brother, and Sister-in-Law** for always providing me the moral and emotional support. I am thankful to my sweet **nephew** for always cheering me up when my spirits went low. Without my family's support and love, I would never have finished this research work.

Hina Abbas

ABSTRACT

Phosphorus is an important macroelement that regulates crop health, grain yield, and productivity. Increasing demand for phosphorus fertilizer, unfertile soils, limited resources of poor farmers, and depleting reservoirs of natural phosphorus are among the major problems of phosphorus deficiency. Wheat crop is mostly grown on marginal lands and rainfed areas, where phosphorus content is lower, and P fixation is limited. The development of wheat varieties with a deep rooting system, nutrient-use efficiency, and high yielding under phosphorus starvation condition is the sole solution to improving wheat productivity. To develop such wheat varieties, it is necessary to identify the genetic regulators involved in the P use efficiency and deeper rooting. The *Phosphorus Starvation Tolerance 1* (*PSTOL1*) gene has been identified and characterized in rice, maize, and sorghum. This gene is suggested to play a key role in efficient P uptake, deeper rooting, and high yield production under phosphorus starvation. Previous studies in wheat only focused on one homolog, *TaPstol5AS-1,* and characterized its role in phosphorus-use-efficiency. Therefore, the present study was carried out to characterize the *TaPSTOL1* gene at a genome-wide level. We identified the 22 orthologs in the whole wheat genome using the latest reference sequence (IWGSC v.1.1). Based on the phylogenetic tree, these orthologs of the *PSTOL1* gene were classified into three groups. Using RNA-sequence data from a previous study, the expression profiling of 22 orthologs was analyzed in root and shoot tissues under normal and phosphorus-deficient conditions. Four putative candidate genes (TraesCS3A02G018500.1, TraesCS3B02G295000, TraesCS5B02G391900, TraesCS5D02G396800) were selected based on differential expression in shoot and root under control and P starvation condition. RT-PCR further verified the expression pattern of these genes. P-efficient (Pakistan-13) wheat cultivar also significantly increased P-uptake, root length, volume, and surface area compared to P-non-efficient (Shafaq-06) cultivar. Altogether, these results revealed the role of the *PSTOL1* gene in wheat P-uptake, root architecture, and efficient growth of plants under phosphorus starvation conditions. In the future, functional validation of the putative candidate genes in wheat will help us identify the role of the *TaPSTOL1* gene.

INTRODUCTION

1.1 Wheat – Fundamental Food Source Around the Globe

Bread wheat (*Triticum aestivum* L.) is one of the major staple crops around the globe. It is among a few of the largest food crops in the Central West Asia and North Africa (CWANA) region, with a 45% per capita calorie intake and a consumption rate of 200 kg per person annually (Tadesse et al., 2017). It meets about 35% of the calorie demand of the global population, and because of its unique ability to make many different kinds of foods, wheat tops other primary cereal crops around the world (Shewry and Hey, 2015).

Wheat yield during 1961-2013 increased from 1.1 – 2.6 t/ha (Tadesse et al., 2017). Kazakhstan is the top country that grows wheat on the largest area of about 13.7 Mha, Pakistan is the second with 8.9Mha, and Turkey is the third with 7.9Mha. This increase in the production area and yield were all made possible by the use of improved wheat cultivars obtained from the International Maize and Wheat Improvement Centre (CIMMYT) and the International Centre for Agriculture Research in the Dry Areas (ICARDA) (Tadesse et al., 2017). Wheat is the most produced crop in Asia, one of the most significant food sources in this region, ranking first in China and second in India. According to FAO, wheat is produced 642 million tonnes per year globally. Still, it will not be enough to meet the demands of the increasing population, and by 2050 the global production of wheat will have to be 840 million tonnes per year (Sharma et al., 2015). It is also observed that this production rate declined by >0.9% in recent years, which has become a concern and will become an alarming situation if left unchecked (Gupta et al., 2020).

1.2 Wheat Evolution History

About 10,000 years ago, wheat was domesticated in Fertile Crescent Civilization and became the Neolithic era's founder crops (Avni et al., 2017). Today's hexaploid wheat underwent a polyploidization event about half a million years ago (El Baidouri et al., 2017).

About half a million years ago, two diploid wheat species, *Aegilopes speltoids* (BB genome) and *Triticum urartu* (AA genome), hybridized to form tetraploid wheat *Triticum turgidum* (spp. *diccocoides* - AABB genome) (Bariah et al., 2020). After that,

the second polyploidization event occurred about 10,000 years ago, and *Triticum turgidum* (spp. *durum* - AABB) hybridized with diploid wheat *Aegilopes tauschii* (DD genome) and formed present-day hexaploid wheat (AABBDD) with approx. 17Gbp genome size (El Baidouri et al., 2017) (Figure 1.1). In comparison with their diploid ancestors, the hexaploid wheat multiplied over a wide geographical area. Hexaploid wheat shows an ample number of morphological variations and quickly occupies large diversified ecological niches (Bariah et al., 2020).

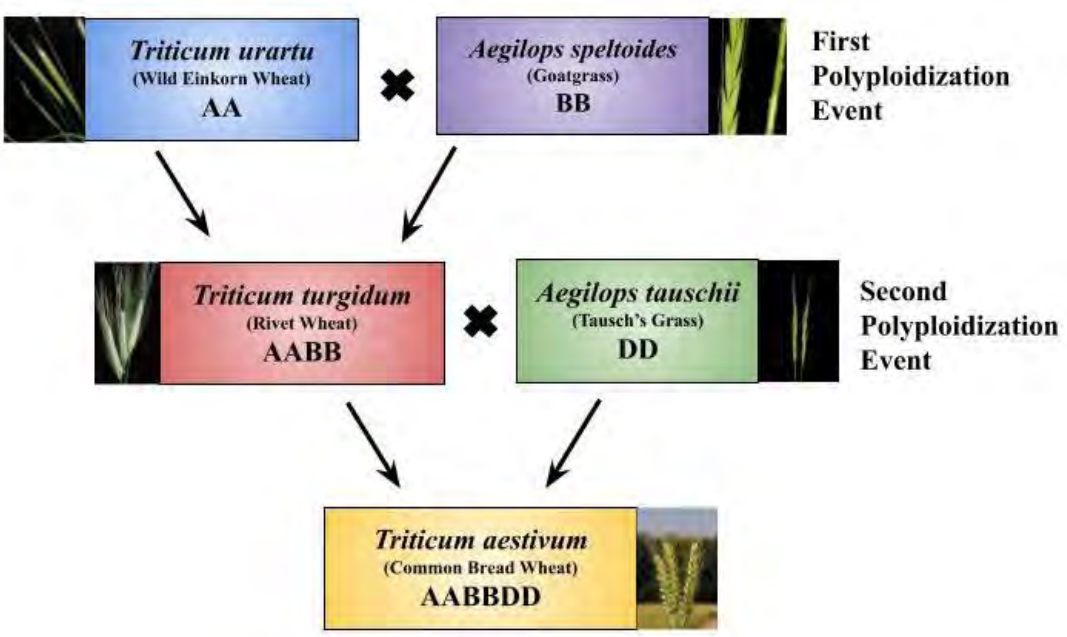

Figure 1.1: Evolution of wheat (*Triticum aestivum L.*) over time. The first polyploidization event occurred about half a million years ago. The second polyploidization event occurred 10,000 years ago.

1.3 Importance of Wheat and Food Insecurity in Pakistan

Pakistan is the 2nd largest country in South Asia in the area and the 36th largest country globally. The primary source of Pakistan's economy is crop production, as out of 79.6Mha of the total area, 19Mha is used for crop production. Wheat is the second most-produced crop in Pakistan. The most dominant food crop is wheat of rabi season, contributing to 1.9% GDP (Ahmad et al., 2015; Haider et al., 2019).

In Pakistan, historically, the food production and population increase have been advancing in equal proportion. But according to recent consensus (Pakistan Gov. consensus 2017), the population has increased to 208 million, and 47% of Pakistan's

population is currently facing food insecurity. It is estimated that by 2050 the population will increase to 270 million, and with escalating water scarcity in Pakistan, maintaining agricultural advancement will become challenging (Khaliq et al., 2019). With Pakistan's increasing population, wheat consumption is escalating at alarming rates, and in the future, wheat and agricultural production will not be able to cope with the increasing population. The season-to-season wheat production is varying from 2391-2848 kg/ha. It suggests that productivity is affected by crop management, bio-physiological factors, deficient soil, and climate changes. These factors cause the yield gap, and with the increasing populous the demand is not being met with every passing year (Khaliq et al., 2019). Hence, the solution will be to either increase the food production in already available geographical areas or develop wheat varieties that can quickly grow even in marginal areas that are deficient and non-suitable for its production.

1.4 Biotic and Abiotic Factors Limiting the Wheat Productivity

The biggest threat to crop plants worldwide is different biotic and abiotic stresses that exponentially affect plant growth and yield. Although plants try to cope by developing different strategies, these stresses still threaten crop yield and biomass. Insects, fungi, bacteria, weeds, nematodes, and viruses entail biotic stress, which causes yield loss of approximately 35% per annum (Baillo et al., 2019). While heat, drought, cold, salinity, water-logging, UV radiation, osmotic stress, and nutrients deficiency are among the abiotic stresses causing yield loss of about 50% annually (Baillo et al., 2019).

Wheat is one of the major food crops in the world that is primarily affected by different biotic and abiotic stresses leading to significant yield loss. Many genes fight against biotic and abiotic stresses, altering plants morphologically, physiologically. Plants also survive by producing different biochemicals to cope with these stresses. A lot of research and experiments are being conducted to identify different biotic stress resistance genes from wild wheat cultivars. Efforts are also underway to develop biotic stress tolerant wheat cultivars around the globe. By far, 450 genes have been identified in wheat, which produces biotic stress resistance. About a third of these genes provide resistance against the four most wheat-damaging fungal diseases; stripe rust, powdery mildew, leaf rust, and stem rust (Singla et al., 2016). Plant hormones like jasmonates, ethylene, auxins, gibberellins, and cytokinins develop tolerance against multiple abiotic

stresses. Hence, these phytohormones can be engineered and modified to produce such lines, which will be abiotic stress-tolerant (Raza et al., 2019).

Among the other abiotic stresses, nutrient deficiency is one of the major hurdles for wheat growth. Factors like economic conditions of different farmers and the surrounding climate of plants affect the nutrient use efficiency of plants. Like other plants, wheat also needs nutrients like N, P, and K to thrive with better yield performance and high-quality fiber (Salim and Raza, 2020). Providing essential nutrients is vital for higher yield and healthy plant growth. Among other nutrients, wheat requires more elevated phosphorus (P) content than other food crops. P-deficiency stress in wheat crops hinders growth and development as it is essential for seed germination, tillering, and seed development. According to an estimate, wheat removes about 2.5 – 8 kg of phosphate per tonne of its grain (Soumya et al., 2021). To keep up with P-deficiency, fertilizers are applied continuously to the soil. It has become difficult, laborious, and expensive to replenish phosphate fertilizers with depleting rock reserves. On top of that, wheat produces a low response against phosphate fertilizers (Soumya et al., 2021). An effort is going around the world to develop such crops that can cope with phosphorus deficiency and survive without losing much yield or biomass because of the phosphorus starvation stress (McDonald et al., 2015).

1.5 Phosphorus Deficiency in Soil and Future Prospects

One of the primary and vital minerals that a plant needs while growing is phosphorus. Phosphorus makes about 0.2% of the dry weight of plants and is a crucial part of the energy unit ATP, phospholipids, and nucleic acids (Hufnagel et al., 2014). The deficiency of available phosphorus is one of the major abiotic stresses in the process of plant growth. A lot of phosphorus is present in tropical soil. Still, its bioavailability is relatively low because most of the phosphorus is fixed in the soil clay by iron oxides, aluminum, or in the form of organic compounds (Hufnagel et al., 2014).

To increase the bioavailability of phosphorus and overcome its deficiency in the soil, fertilizers are applied to the soil regularly. These fertilizers are made from phosphorus rock reserves, which are the non-renewable mineral source, and this reserve keeps depleting at a much faster rate. According to some studies, most phosphorus rock reservoirs will only last for the next 300-400 years while, according to others available, phosphorus will be gone by 2100 (Sattari et al., 2012; Veneklaas et al., 2012). With the

depleting phosphorous rock reserves, the processing, manufacturing, and transportation costs are skyrocketing (Gemenet et al., 2016). This makes it difficult for farmers of developing countries to afford phosphorus fertilizer in the future. This emphasizes the development of varieties which will perform better under phosphorus-deficient conditions.

1.6 Effect of Phosphorous Deficiency on Crop Plants

The deficiency of available phosphorous dramatically affects the yield and morphology of the plants. Under phosphorous deficient soils, the shoots of the plant stop growing or develop at a prolonged rate. Plant roots become more extended, dry root weight and root surface area increase, and root diameter decrease (UYGUR and Mustafa, 2018). Some plants secrete mucilage in phosphorous deficiency, while growing conditions also affect the response against phosphorous deficiency (UYGUR and Mustafa, 2018). Different cultivars show diverse responses against phosphorous deficiency. According to (Chaudhary et al., 2008), there was a severe decrease in photosynthetic capability, biomass, and nitrogen fixation ability in the mashbean and mungbean.

When grown hydroponically in a phosphorous deficient condition, barley plants (Hordeum vulgare) showed an increase in root to shoot ratio, decrease in shoot weight, biomass, and tillering, and a minor reduction in chlorophyll content (Frydenvang et al., 2015). The first step in the electron transport chain, in which electron flows from cytochrome to electron sink, completely vanished under phosphorous deficient conditions, indicating the significant effect of P deficiency on the photosynthesis ability of barley plants (Frydenvang et al., 2015). P-deficiency in barley (*Hordeum vulgare)* showed no visible symptoms on leaves but damaged the leaf tissue internally to a great extent. It caused a reduction in orthophosphate concentrations in the stroma of chloroplast, which inhibited the activity of ATP synthase. This leads to proton accumulation and lumen acidification, inhibiting the electron transport chain (Carstensen et al., 2018). In rice (*Oryza sativa*), the phosphorous deficiency caused a reduction in nodal root numbers, plant phosphorous content, dry weight of shoots, plant height, and plant tiller numbers. These rice plants also exhibit a decline in the density of large lateral roots and root length of both large and small lateral roots, along with an increase in thickness and length of root hairs (Vejchasarn et al., 2016).

Hence, the need for such cultivars adept at growing appropriately under phosphorus-deficient conditions to attain sustained agricultural production globally. In West Africa, multi-environmental trials were conducted to introduce new agronomic practices in *Sorghum bicolor* to grow better in a phosphorous deficient environment (Leiser et al., 2012). Similarly, sugarcane varieties were grown under the phosphorous deficient conditions to understand the difference in photosynthetic activities and morphological parameters and identify which cultivars are better suited for growth in phosphorous deficient environments (Zambrosi et al., 2015).

1.7 Impact of Phosphorous Deficiency on Wheat

Like other crops, the phosphorous deficiency in the soil also affects the wheat crops significantly. The phosphorous fertilizer application is essential for the high yield and optimum quality of produced wheat under phosphorous deficient conditions. With the depleting phosphate rock reserves and side-effects of fertilizer, there is a dire need to develop wheat cultivars that can grow under poor phosphorous soils (Yang et al., 2018).

Roots are the central passage through which a plant acquires all its minerals and water from the soil, which makes wheat plant roots the best target for modification for growing in nutrient-deficient soils (Stangoulis, 2019). To correctly modify the wheat root system to make it self-sufficient in phosphorous deficient soils, we need to understand the root architecture system of wheat plants. Wheat has many adventitious and seminal roots (Stangoulis, 2019). Eighty-nine wheat genotypes were investigated under low phosphorus content (5μM) and high phosphorus content (500μM), which revealed a significant increase in surface area, total root length, root volume, root to shoot ratio, and total root dry weight (Soumya et al., 2021). The reduction in root diameter and phosphorus uptake was observed as well. By identifying and targeting genes responsible for different root morphology under phosphorous stress in wheat cultivars resistant to deficient soils, we might modify wheat cultivars to better adapt to phosphorous deficient soils without a decrease in yield.

1.8 Plants Adaptive Strategies Against Phosphorous Deficiency

To cope with P-deficiency stress plants, undergo many morphological, physiological, and biochemical changes. Morphologically, plants alter their root architecture to increase phosphorus use efficiency (PUE). They release several low-molecular organic compounds to increase phosphorous uptake from the soil and form a mutual

relationship with mycorrhizal fungi and growth-boosting bacteria (Malhotra et al., 2018). Legumes create a symbiotic relationship with rhizobia to maintain phosphorous homeostasis as a strategy against P deficiency. They keep stable amounts of phosphorous in their tissues by developing phosphorous sinks in nodules, allocating elevated phosphorous to nodules, or acquiring phosphorous directly through nodules surface (Sulieman and Tran, 2015). Maize showed enhanced root cortical aerenchyma (RCA), reducing root aspiration and increasing P uptake efficiency (Vejchasarn et al., 2016). To prevent the inhibition of photosynthesis under P deficiency, plants alter the composition of thylakoid membranes. It does not require membrane-bound inorganic phosphate, leaving it accessible for photosynthesis (Malhotra et al., 2018).

1.9 Molecular Response of Plants Towards P-Deficiency

Along with morphological responses, plants show many molecular responses to cope with P deficiency in the soil. Plants have evolved by creating a large and diverse rhizospheric pool to have hefty inorganic phosphate uptake by releasing P-releasing enzymes like RNAses, Purple Acid Phosphatases (PAPs), and excreting high amounts of organic acids (Lan et al., 2018). Plants have reprogrammed their metabolism to increase P use efficiency, and they also regulate the production of high-affinity phosphorous transporters to control the inflow of extracellular inorganic phosphate (Lan et al., 2018).

Plants induce membrane transporters to enhance their phosphorous acquisition capability (Chen et al., 2015). Some plants use different phosphatases and organic acids to increase phosphorous uptake from soil and mobilize the internal phosphate molecules. It was observed that immature mulberry leaves display a defense mechanism to protect them from oxidative damage caused by P deficiency by increasing the activity of their antioxidant enzymes (Chen et al., 2015).

1.10 Genes Involved in Producing Phosphorus Stress Response

Many genes are involved in generating responses toward P deficiency. These genes are divided into two groups; "early genes," which show rapid and non-specific response towards P deficiency, and "late genes," which are activated under prolonged P deficiency and influence the metabolism, morphology, and physiology of plants to cope with P deficiency (Hammond et al., 2004). The genes responsible for generating responses toward phosphate starvation stress are termed PSR genes or Phosphate

starvation responsive genes (Kuo and Chiou, 2011). Many factors are found in plants that regulate these PSR genes, with microRNA being the new player. The microRNAs are involved in regulating Pi homeostasis in plants and signaling during P deficiency (Kuo and Chiou, 2011).

Constant research is being conducted to identify phosphorous regulation genes. Two cis-regulatory elements were identified upon analysis of P regulation genes in yeast which were involved in controlling gene expression against P deficiency. Similar factors were then identified in P deficiency responsive genes of tomato (*TPSI1*), the (barrel clover) *Medicago truncatula* (*Mt4*), *Arabidopsis thaliana* (*At4* and *AtIPS1*), and in *Oryza sativa* (*OsPI1*). These genes encode short open reading frames and induce rapid P deficiency-specific response (Hammond et al., 2004). Pht1 family of proteins Finger Millet (*Eleusine coracana* L.) plants show promising results under phosphorous stress. The expression of *EcPT1-4* in Finger Millet crop plays a significant role in a phosphorous acquisition under P-deficient conditions (Pudake et al., 2017). Genes encoding phosphate transporter proteins were found to be involved in coping against phosphorous stress by generating the symbiotic relationship with ectomycorrhiza in Masson pine (*Pinus massoniana*) (Zhang et al., 2017).

1.11 Role of *PSTOL1* (*Phosphorous Starvation Tolerance 1)* Gene under Phosphorous Stress

Among other P deficiency tolerance-inducing genes, *PSTOL1* is one of the critical genes. The Pup1 specific protein-kinase was discovered by (Gamuyao et al., 2012) and named as phosphorous starvation tolerance 1 (*PSTOL1*) gene in rice (*Oryza sativa*). It was found that when the *PSTOL1* gene was over-expressed in plants growing in phosphorous deficient soil, a significant increase in yield and biomass of rice grains was observed. *PSTOL1* gene acts by increasing the early growth of roots, enabling the plants to acquire more phosphorous from P deficient soil (Gamuyao et al., 2012).

Upon comparing rice crops that were overexpressing *PSTOL1* and those lacking the gene, it was seen that crops with overexpression showed enhanced root growth and proliferation; hence, the kinases coded by the *PSTOL1* gene increased the ability of plants to mine more phosphorous (Kochian, 2012). The finding of the *PSTOL1* gene opened up new frontiers of research. By identifying orthologs of this gene in different crops and targeting its expression, crops can be made to proliferate in phosphorous

deficient soil with more yield and biomass. The use of fertilizer can also be reduced for inorganic phosphorous acquisition.

PSTOL1 homologs were identified and investigated in Sorghum bicolor to create such Sorghum lines that can grow with more yield and biomass under P deficiency stress. An experiment was conducted in Brazil; root surface area and root length were correlated with grain yield. When *PSTOL1* homologs were targeted, the root diameter decreased, and the roots surface area increased, thus leading to a significant increase in yield (Hufnagel et al., 2014).

Like Sorghum bicolor experiment, our study aims to identify orthologs of the *PSTOL1* gene in wheat through sequence alignment. Those orthologs can be targeted to make wheat cultivars resistant to phosphorous deficiency in the soil, producing a high yield of grains under P-deficient soils. This study aims to reduce the use of phosphorous fertilizers, preserve the continuously depleting phosphate rock reserves, and build better wheat cultivars capable of growing and thriving even in deficient conditions.

1.12 Objectives

Present study had following objectives;

- Genome-wide identification of *PSTOL1* gene ortholog in wheat (*Triticum aestivum L.*)
- Morphological evaluation of lines against phosphorus effective uptake and root architecture
- Molecular characterization of putative genes and identification of candidate key regulator genes for *OsPSTOL1* gene.

MATERIALS AND METHODS

2.1 Sequence Retrieval and *PSTOL1* Orthologs Identification in Wheat

The *PSTOL1* nucleotide and protein sequence of *Oryza sativa* were retrieved from NCBI (GenBank: QIN51176.1). The *PSTOL1* sequence was used as a query sequence for BLASTP and BLASTN. EnsemblPlants was used for BLAST against *Triticum aestivum L.* to identify *PSTOL1* orthologs in wheat. Duplicate hits were removed, and the cut-off values of identity >50% and *E-value* (1e-5) were used for sequence reliability. In total, 48 orthologs were selected.

The *PSTOL1* protein sequence was also used to BLASTP against four closely related species (*Brachypodium distachyon, Arabidopsis thaliana, Sorghum bicolor, Zea mays,* and *Oryza sativa)* to find the orthologs and evolutionary relationship among those species and wheat. BLASTP was performed on EnsemblPlants, and 8 orthologs were selected from *Brachypodium distachyon*, 3 from *Arabidopsis thaliana*, 17 from *Sorghum bicolor*, 9 from *Zea mays,* and 3 from *Oryza sativa* by keeping the cut-off value of *E-value* = 1e-5 and identity >80%.

2.2 Domain, Motifs, and Gene Structure Analysis

The default mode of SMART tool (Letunic and Bork, 2018) and MEME Version 5.3.3 (Bailey et al., 2015) were used to predict conserved domains and motifs in the identified 48 *PSTOL1* orthologs in wheat. The classic mode was used in the MEME suite to find 20 maximum motifs in one sequence and zero or one occurrence per sequence.
Sequences were filtered after domain analysis, and 22 sequences were kept that had the conserved Ser/Thr kinase domain (Pfam identifier PF00069.18) of the protein kinase family. GSDS2.0 online tool was used to draw gene structure of selected sequences (Hu et al., 2015). TBtools software was used to illustrate the motif, domain, and gene structure patterns (Chen et al., 2018).

2.3 Phylogenetic Tree Construction and Promoter Analysis

ClustalW was used to perform protein sequences alignment of 22 wheat and orthologs from other species (Thompson et al., 2003). The alignment was further used to build a phylogenetic tree using the neighbor-joining (NJ) method with 1000 bootstrap replication in MEGAX software (Kumar et al., 1994). The annotated mid-rooted tree was illustrated using iTOL (Letunic and Bork, 2021).

Cis-regulatory elements were identified in the promoter sequences of 22 orthologs. For this purpose, upstream sequences of about 1500bp were downloaded from the EnsemblPlants database. The online tool PlantCARE (Lescot et al., 2002) was used to identify cis-elements in the upstream promoter sequences. The results were visualized as a heatmap in TBtools.

2.4 Duplicates Identification and Gene Location among Wheat Accessions

Tandem and segmental duplicates were identified among 22 wheat orthologs. The following criteria were employed to select tandem and segmental duplicates genes:

1. Alignment score > 80%
2. Identity > 80%
3. Threshold < 10^{-10}
4. Located on different chromosomes
5. Located on the same chromosome
6. Distance between the genes was not more than 25Kb

Genes that satisfied the first four criteria were designated as segmental duplicates. In contrast, genes that followed the last two criteria (5-6) were selected as tandem duplicates. From the wheat reference sequence (IWGSC 1.1), the chromosome lengths and gene positions were taken. These positions with segmental duplicates were visualized using TBtools.

2.5 Ka\Ks Analysis within Genome and with Other Species

The coding sequences of the identified segmental duplicates were acquired, and multiple sequence alignment was conducted using CLUSTALW. In-house Perl script was built based on ParaAT 2.0 to back translate the multiple sequence alignment into axt format (as accepted in Ka\Ks calculator) (Zhang et al., 2012). After getting the alignment in the required format, the Ka\Ks (nonsynonymous per synonymous substitution rates) were calculated with Nei and Gojobori method using the KaKs 2.0 calculator (Wang et al., 2010). The divergence time between duplicated genes was calculated by T = Ks/2r (Tyagi et al., 2020).

2.6 Synteny Analysis with Ancestral Plants

Proteomes and GFF3 files of four wheat ancestors (*Triticum urartu, Triticum dicoccoides, Triticum turgidum, Aegilopes tauschii*) were downloaded from the

EnsemblPlants database. Proteome and GFF3 file for *Triticum aestivum L.* was downloaded from the IWGSC wheat database (iwgsc_refseqv1.1 2017) (Alaux et al., 2018). BLASTP was conducted for all five proteomes on Linux with in-house scripting. BLAST and GFF3 files were further used to predict collinearity through the MCScanX algorithm (Wang et al., 2012). Segmental duplicates were further identified from the collinearity file. Self-syntenic and ancestral gene pairs were visualized in Advanced Circos using TBTools.

2.7 Meta-QTL Analysis

To identify the localization of *T. aestivum PSTOL1* orthologs with QTLs for morpho-physiological and biochemical traits under phosphorus starvation, QTLs and linked molecular markers were retrieved from previous publications (Shi et al., 2008; Guo et al., 2012; Ren et al., 2017; Yuan et al., 2017; Yuan et al., 2020; Yang et al., 2021). To obtain the physical position, each marker sequence or marker name was BLAST against the GrainGenes database (Blake et al., 2019). *TaPSTOL1* orthologs were co-localized with phosphorus stress-related QTLs were displayed by using MapChart software (Voorrips, 2002). QTLs co-localized with the *TaPSTOL1* orthologs were 184 visualized by red color.

2.8 RNA-seq Data Collection and Primer Designing

RNA-seq data were retrieved from the previous study of (Oono et al., 2013) from the wheat expression browser (Borrill et al., 2016). Expression data of 22 orthologs was acquired from the expression browser. Expression data as TPM values was collected from multiple experiments of roots and shoots at the vegetative stage in both control and phosphorus-treated plants.

TPM values were used to generate a heatmap in TBtools. The up-regulated and downregulated genes were selected for further expression profile confirmation in the studied cultivars. Selected gene expression primers were designed using Primer-BLAST of NCBI (Ye et al., 2012). Primer melting temperature was set to 57° minimum and 60° maximum, and PCR product size was set to minimum 80 and maximum 130. The rest of the parameters were kept on default (Table 2.1)

Table 2.1: List of primers for expression profiling

S. No.	Gene	Primer Name	Primer Seq.
1	TraesCS3A02G018500.1	P3A500-F	TCTGAAGGAATGAGACGGGC
	TraesCS3A02G018500.1	P3A500-R	TTGGGTGCTAGGAGTTGTCG
2	TraesCS3A02G261800.5	P3A800-F	TCTCTTGATATGCCACCGGC
	TraesCS3A02G261800.5	P3A800-R	TGATTCAGGCACATGGAGGG
3	TraesCS3B02G295000.1	P3B5K-F	CCAGCACCTCCACTTCAACT
	TraesCS3B02G295000.1	P3B5K-R	TGAGGCGTTCTTCTTGCAGT
4	TraesCS5B02G391900.1	P5B900-F	ATCTCAGATGCTGCCATCCC
	TraesCS5B02G391900.1	P5B900-R	GCTCCAGTCAGCTGCTATGT
5	TraesCS5D02G396800.1	P5D800-F	TTCCCTCTCCAGCTCCTTGA
	TraesCS5D02G396800.1	P5D800-R	TGATGGTGTCTTGGCCTGAG

2.9 Pot Experiment for Morphological Evaluation

Two wheat varieties, Pakistan-13 and Shafaq-06, were selected to understand the phosphorus-deficient response at the morphological level. The seed surface was sterilized with Clorox and thoroughly washed with distilled water. Seeds were then incubated overnight on moistened filter paper in Petri plates to break the seed dormancy. After 2-3 days, the seedlings were shifted in the labeled plastic bags. The plastic bags were filled with soil mixture, including soil: sand at a ratio of 2:1. Each bag had one seedling in it with 5 replicates. The seedlings were then grown for about 15 days with given tap water after every 1 or 2 days.

After a fortnight, the phosphorus treatment was initiated. Control plants were given normal tap water; phosphorus sufficient plants were watered with 0.5mM KH_2PO_4 solution, and the plants grown in phosphorus-deficient environments were irrigated with 0.05mM KH_2PO_4 solution (Wang et al., 2019). The treatment was given for 15 days. After 15 days, plants of each treatment were harvested, and different morpho-physiological traits were taken.

2.10 NDVI Measurement

Plant health was calculated by measuring all plants' NDVI (Normalized Difference Vegetation Index) (Moriondo et al., 2007). The GreenSeeker® handheld crop sensor was used for taking the values under intense and visible sunlight. Three observations of NDVI were taken from each plant.

2.11 Chlorophyll Content Measurement

The first leaves of all the plants were taken for chlorophyll content measurement. Three biological and three technical replicates were taken for chlorophyll content estimation. Chlorophyll content was measured by chemically extracting the chlorophyll from leaves using the method proposed by (Arnon, 1949).

The leaves were crushed in 5ml (80%) acetone and then shifted to 50 ml falcon tubes. The total volume of 80% acetone was made up to 10ml. The falcon tubes were then centrifuged at 5000 rpm for 15 minutes. The supernatant was taken, and the pellet was discarded. The supernatant was filtered once for further purification. The chlorophyll a, b and carotenoids content in the samples were then measured by spectrophotometer at 470nm, 646nm, and 663nm.

The chlorophyll a, b and carotenoid content were then calculated using equations (Lichtenthaler, 1987);

- $Ca = 12.25A_{663.2} - 2.79A_{646.8}$
- $Cb = 21.50A_{646.8} - 5.10A_{663.2}$
- (Total chlorophyll) $Ca+b = 7.15A_{663.2} + 18.71A_{646.8}$
- (Carotenoids) $Cx+c = 1000A_{470} - 1.82\ Ca - 85.02\ Cb / 198$

2.12 Morphological Parameters

Tillers per plant and shoot length were measured from 3 observations of control and phosphorus treatment. Plants were harvested from three bags of each treatment, while the remaining two bags were used for RNA sampling. The plastic bags were cut very carefully with scissors such that none of the plant material was destroyed and the roots remain intact thoroughly. Plants along with soil were taken out of bags with care and placed on a very fine sieve. The soil was removed with hands from the roots with extreme care without breaking any roots. Roots were then washed with extreme caution and effort to remove all the remaining soil and debris.

After harvesting, roots were placed on filter paper to absorb the water. After drying off, the roots were separated from the shoot at the base. Parameters like root length, fresh shoot weight, fresh root weight were measured, and after drying in a hot air oven at 70°C for 2 days, dry shoot and root weight were also measured by a sensitive measuring balance.

2.13 High-throughput Root Phenotyping

The washed and cleaned roots were placed in the root scanning glass tray (8 x 12 inches). The tray was filled with water to spread the roots evenly. Roots were scanned using hp® Scanjet 5590 scanner at a grey-white scale and 300 dpi resolution.
The images were used to find root traits using RhizoVision Explorer – interactive software for generalized root image analysis (Seethepalli et al., 2020). Root traits like total root length, average diameter, root volume, and root surface area were calculated using this tool.

2.14 Phosphorus Content Measurement

Phosphorus content was measured from the root and shoot tissues of all treated plants. Three independent samples from each biological replicate were taken as technical replicates to make precise phenotyping. About 0.25 g tissue sample was weighed for each sample. The samples were further droved in glass tubes and placed in a digestion machine for breakdown. The digested samples were then analyzed to quantify phosphorus content using an atomic absorption spectrometer (Shar et al., 2002). Raw data were used to calculate the P concentrations that were expressed in mg/kg dry weight.

2.15 Plant Sampling for RNA Extraction

Two observations from each treatment of a cultivar were retained for RNA sampling. Plants were carefully harvested as described above. After proper washing, plant roots and shoots were sprayed with 70% ethanol to remove any foreign contamination. 1st leaf and primary roots of each plant were cut down with sterile scissors. Samples were enveloped in aluminum foil and immediately placed in a liquid nitrogen container. Samples were labeled and stored at -80°C.

2.16 Total RNA Extraction

RNA extraction from the root and shoot samples was performed using TRIzol® reagent for RNA purification. TRIzol protocol used was according to (Simms et al., 1993). Sterile mortar and pestle were cooled with liquid nitrogen. Samples were placed in a cooled mortar and pestle (autoclaved at 121°C and 15psi pressure for about 2 hours) and ground with liquid nitrogen into fine powder. 1ml of TRIzol was added into 1.5ml Eppendorf tubes. Eppendorf tubes were placed on ice, and about 2g of ground tissue sample was added to the TRIzol. Tubes were vortexed for few seconds and centrifuged at 4°C at 12,000g for 10 minutes. The supernatant was collected in another sterile tube, and 200µl chloroform was added, tubes were inverted few times and incubated for 5 minutes at room temperature.

Eppendorf tubes were then centrifuged at 4°C for 15 minutes at 10,000g. The upper aqueous phase was collected in a sterile tube, and the pellet was discarded. 300µl chilled isopropanol and 300µl of Na-Citrate solution were added to, tubes were inverted few times for proper mixing and incubated at room temperature for 5 minutes. Tubes were then centrifuged at 4°C at 10,000g for 10 minutes. The supernatant was discarded, and the pellet (hardly visible) was washed with 1ml of 75% ethanol, vortexed for few minutes, and centrifuged at 4°C at 10,000g for 10 minutes. Ethanol was carefully and thoroughly removed from the tubes. The pellet was dissolved in 30µl of nuclease-free water.

2.17 Extracted RNA Confirmation and Quality Validation

To identify the pellet contained RNA and check the quality of RNA, the dissolved pellet was run on gel electrophoresis and visualized on Gel Doc.

2.17.1 Stock Buffer Preparation

For making 1000ml/L buffer, 20ml of 50X TAE buffer was dissolved in 980ml of distilled water.

2.17.2 Gel Preparation

To prepare 1% gel, 70ml of 1X TAE buffer was taken from stock, 0.7g of agarose was measured using a weighing scale, and was dissolved in the buffer by heating for 1 minute. The gel was cooled down for few minutes, and 4µl of ethidium bromide

(carcinogenic) was carefully added. The gel was cooled down to room temperature and poured into a gel tray with an attached comb.

2.17.3 Sample Loading

After the gel was set, the tray was placed in an electrophoresis tank filled with 1X Tae buffer. The gel was immersed in the buffer and comb removed. 3µl of 1Kb DNA Hyper Ladder (Gene Ruler^{TM}1000bp DNA ladder Thermo Scientific) was loaded in the first well. 3µl of loading dye (Thermo Scientific 6X DNA loading dye) was mixed with 4µl of each sample, and then every sample with dye was loaded in wells one by one. The time for electrophoresis was set for 10 minutes with 200 Voltage and 300 Amp current.

2.17.4 Gel Visualization

The gel was visualized using Invitrogen™ iBright™ FL1500 Imaging System. The gel was carefully placed on the tray. The gel was observed under smart exposure to confirm the presence and quality of RNA.

2.18 RNA Quantification

Nanodrop was used to quantify the amount of RNA in the extract. 1µl of the sample was taken and placed on the lens of Biospec™ (Biospec Nano spectrophotometer for Life Sciences). Three readings were taken for the reliability of each sample, and the RNA was quantified in ng/ul concentration with O.D at 260/280nm and 260/230nm.

2.19 cDNA Synthesis

Thermo Scientific Revert Aid – Reverse Transcriptase kit was used for constructing cDNA from extracted RNA. The synthesis of cDNA was carried out in the following steps; Mathematical calculation was done to achieve the final concentration of RNA in 1000ng from the mean values of RNA concentration. After the calculations, the varying amounts of RNA and 1ul OligodT Primer were added to PCR tubes and incubated at 65°C for 5 minutes in ProFlex™ 3x32 wells PCR system by Applied Biosystems® Thermal Cyclers.

The PCR master mix was prepared with constant ingredients; 2ul dNTPs, 4ul RT buffer, 1ul Reverse Transcriptase enzyme, and making up to 7ul of master mix for each PCR tube. After the incubation, the PCR tubes were placed on the cold rack (4°C) for 1 minute. Proceeding, the master mix was added to each tube and put back in the PCR. Tubes were incubated at 42°C for 1 hour, with an extension done at 72°C for 7-10

minutes. After 1 hour and 15 minutes, the PCR tubes containing cDNA were removed and stored at -20°C.

2.20 Real-Time Quantitative PCR (qRT-PCR)

Real-time quantitative PCR (Applied Biosystems® 7900 HT Fast RT PCR) with StepOnePlus software were used to check the expression of the identified orthologs under-treated and control conditions. There were 3 negative controls, and Actin acted as an endogenous control. Taq Man SYBR-Green kit was used for conducting RT PCR. For 1 Tube in RT PCR strips, a total 10ul reaction mixture was added; 1ul cDNA, 5ul SYBR-Green, 3.6ul Water, and 0.2ul of each forward and reverse primers (Table 2.2).

Table 2.2: Temperature variations of RT PCR steps

Stage	Temperature	Time
Denaturation	94°C	10 Minutes
40 Cycles	95°C	30 Seconds Each
Annealing	58°C	30 Seconds
Extension	72°C	30 Seconds
Melt Curve	95°C	15 Seconds
Stage 2 Melt Curve	60°C	1 Minute

After the PCR, amplification plots, melt curves, and ΔCT values were taken for further analysis.

2.21 Statistical Analysis

Bar charts were made in Excel v.2019 and Origin for all morphological, physiochemical, and biochemical parameters to demonstrate the descriptive statistics. To understand the genetic variations among studied traits of both genotypes under phosphorus and normal conditions and significant impact of treatment were subjected to the analysis of variance. The factorial analysis of variance was carried by using statistics v8.1 software. All morphological traits were correlated using "correlate" and "agricolae" packages in R.

RESULTS

3.1 Sequence, Motif and Gene Structure Analysis with Identification of *PSTOL1* Orthologs in Wheat

After the sequence similarity search on the EnsemblPlants database, a large gene family was hit, having approximately 103 members. Based on the set threshold (>50% and 1e-5), 48 orthologs were filtered and selected from BLASTN and BLASTP. According to the similarity, the most similar orthologs of *OsPSTOL1* were found on chromosome 3B with 92% identity. The second most similar orthologs were on 6A the 6D and 3A with the identity of 90% and 89%.

The conserved domain in the *PSTOL1* gene of *Oryza sativa* is reported to be S_TKc (Ser/Thr Kinase) (UniProtKB-A0A0H3VD96). All 48 orthologs, when searched against the SMART database, 22 were found to have S_TKc domain, along with that 11 orthologs had GUB_WAK_bind domain, which is a cysteine residue rich wall-associated receptor, galacturonan binding kinase domain. This domain is the extracellular component of the S_TKc domain and binds to the pectin in the cell wall. While 9 orthologs also had a WAK_association domain on the C terminal of the GUB_WAK_bind domain (Figure 3.1).

The 22 wheat *PSTOL1* orthologs were searched against the MEME suite for identifying 20 conserved motifs. 6 motifs were found to be part of the functional and conserved S_TKc domain. Motif 20, only predicted in 6 orthologs, was part of the GUB_WAK_bind domain, and motif 9,11 and 18 were also part of the GUB_WAK_bind domain in 3 orthologs. Motif 8 and 10 were related to the WAK_association domain in 3 orthologs (Figure 3.1).

Phylogenetic tree was constructed, using MEGAX, of identified genes to understand their evolutionary relationship and to identify the structural diversity of *PSTOL1* wheat orthologs, gene exon/intron structures were determined using GSDS 2.0. It was found that all orthologs contained introns, with 1 ortholog containing 1 intron, 13 orthologs containing 2 introns, 7 orthologs had 3 introns, while 1 ortholog had 4 introns. Variations among the intron numbers are probably because of the functional differentiation of these orthologs. Additionally, 8 orthologs had (UTRs) untranslated regions (Figure 3.1).

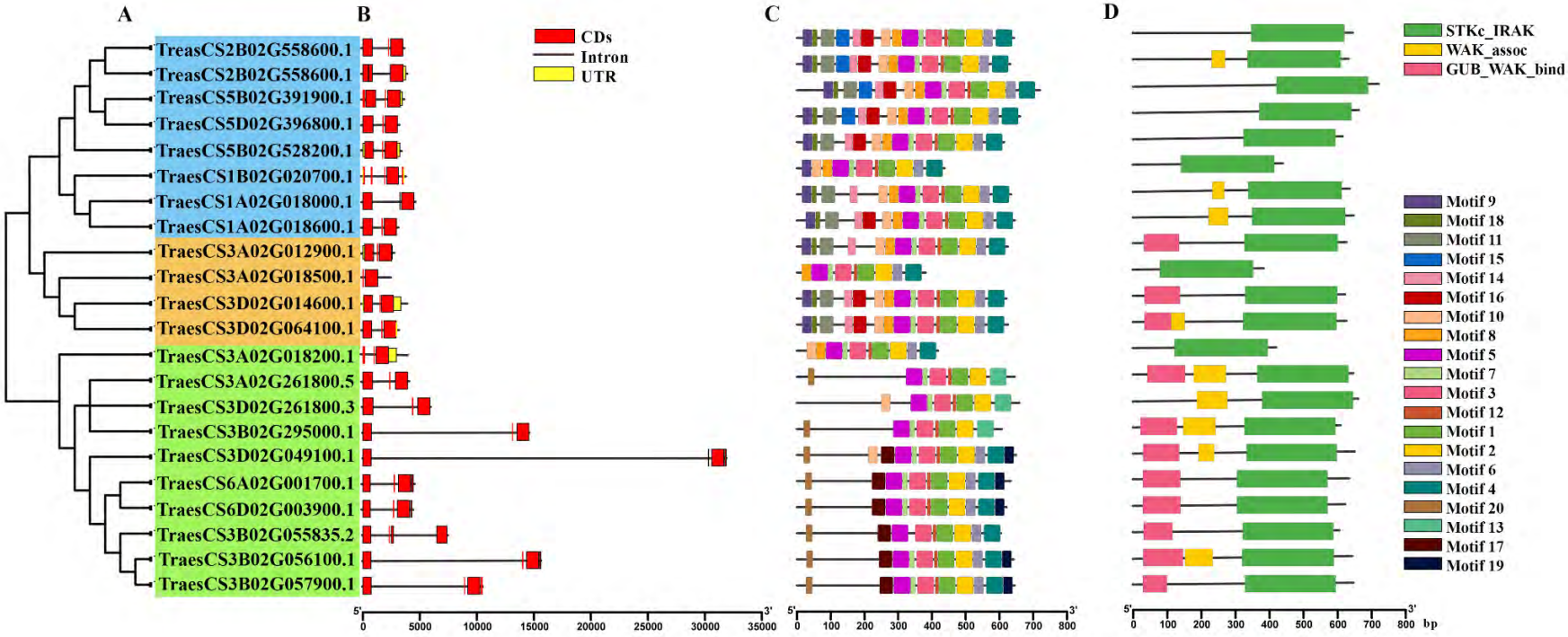

Figure 3.1: Gene structure, motif, and domain analysis image designed on TBtools. **(A)** phylogenetic tree constructed on MEGA 7.0 with 1000 bootstrap replications with Neighbor-Joining method **(B)** exon, intron, and UTRs analysis done on GSDS 2.0. with red boxes displaying CDs, solid black lines depicting introns, and yellow boxes representing UTRs **(C)** 20 conserved motifs were identified using the MEME tool. Each motif is shown with different color **(D)** Conserved domains identified using the SMART tool. The green rectangle represents the S_TKc domain, pink represents the GUB_WAK_bind domain, and the yellow rectangle represents the WAK_association domain.

3.2 Cis-Regulatory Elements Analysis of Promoter Regions

Differences in gene regulation and function can be understood by identifying cis-elements and their distribution patterns in the promoter region of such genes. After identifying cis-elements in the 1500bp upstream promoter regions of the wheat *PSTOL1* orthologs, it was found that 24 cis-regulatory elements were involved in biotic and abiotic stress, 7 in growth, and development, while 10 in phytohormone response.

As seen in (Figure 3.2), the cis-element G-Box, which is involved in the biotic and abiotic response, and the ABRE element involved in phytohormone response, are distributed in almost all orthologs with G-Box lying in maximum number in (TraesCS3D02G014600.1) gene. After that, both G-Box and ABRE elements are present in the second maximum concentration in the (TraesCS3D02G261800.3) gene. Following the pursuit, phytohormone response producing elements (CGTCA motif, TCACG motif) and growth and development responsive CAT-box are also distributed among most orthologs. Contrary to this, among biotic and abiotic responsive elements (ATCT-motif, I-box, chs-CMA2a, GA-motif, ATC-motif, Box II, CAG-motif, GTGGC, and LAMP-element), among growth and development responsive elements (circadian, HD-Zip 1, MSA-like, and RY-element) and the phytohormone response generating elements (TGA-box) show decreasing distribution among all orthologs.

3.3 Phylogenetic Analysis of *PSTOL1* Orthologs with other Related Species

To understand the evolutionary relationship of wheat with other closely related species the *OsPSTOL1* gene sequence was used to find orthologs in related species like *Brachypodium distachyon, Arabidopsis thaliana, Sorghum bicolor, Oryza sativa, Zea mays*. BLASTP identified orthologs in the related species (cut-off values of 1e-5 and identity >80%).

Multiple sequence alignment of 62 sequences (including 22 orthologs from *Triticum aestivum L.*) was conducted on CLUSTALW, and a circular phylogenetic tree was constructed using the Neighbor-Joining (NJ) method and 1000 bootstrap replications (Figure 3.3)

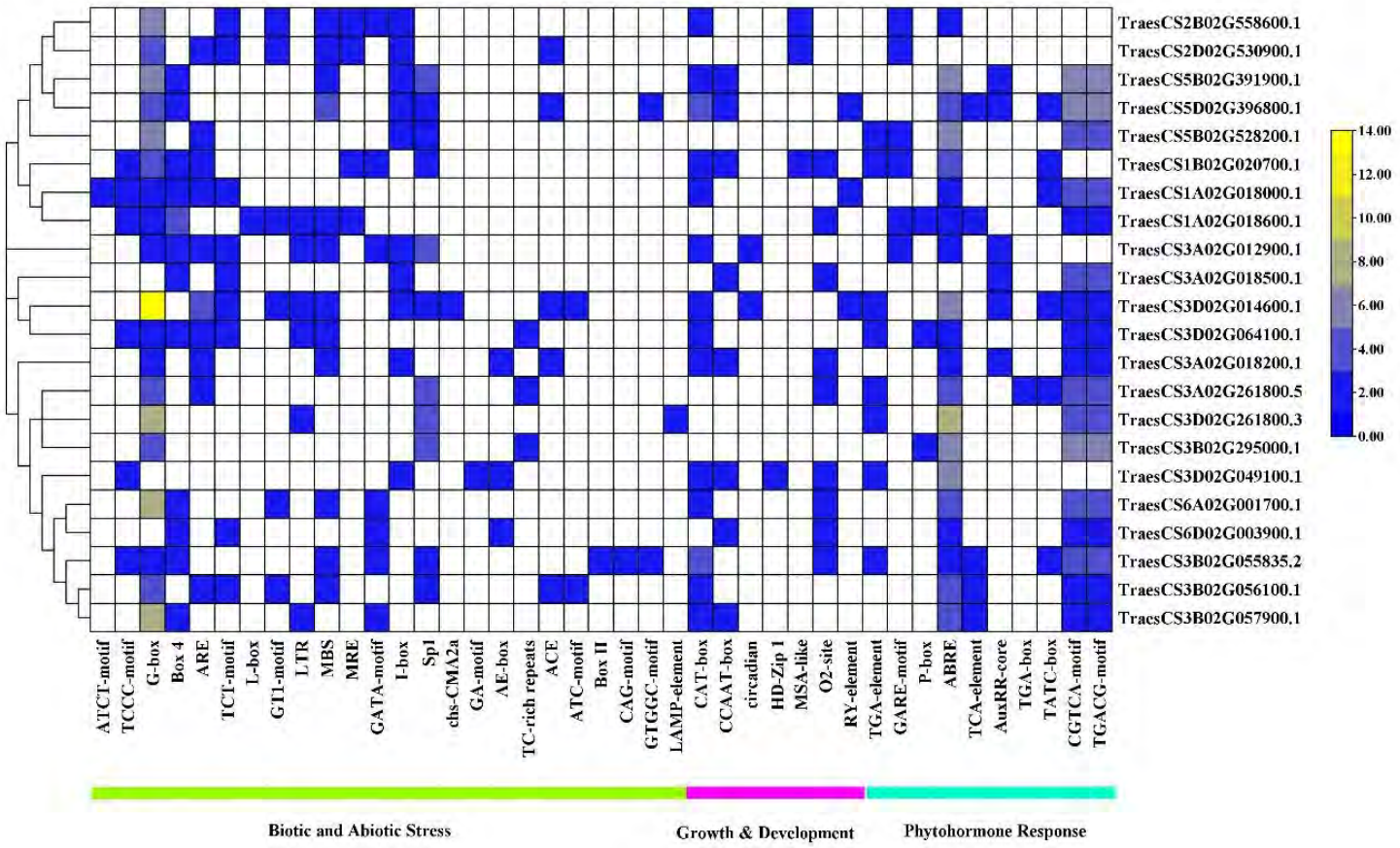

Figure 3.2: Cis-regulatory elements in promoter regions of wheat *PSTOL1* orthologs. The color patterns indicate the distribution of different cis-elements across the ortholog.

The tree was annotated in the iTOL online tool, and it is evident from (Figure 3.3) that *PSTOL1* orthologs in wheat have the closest relationship with *Brachypodium distachyon*, *Sorghum bicolor* and *Arabidopsis thaliana* does not show any association with *PSTOL1* wheat orthologs. According to topology and bootstrap values, the phylogenetic tree was divided into three groups (1,2 and 3), as shown in (Figure 3.3). Group 1 has 26 orthologs, Group 2 has 18 orthologs, and Group 3 has 18 orthologs.

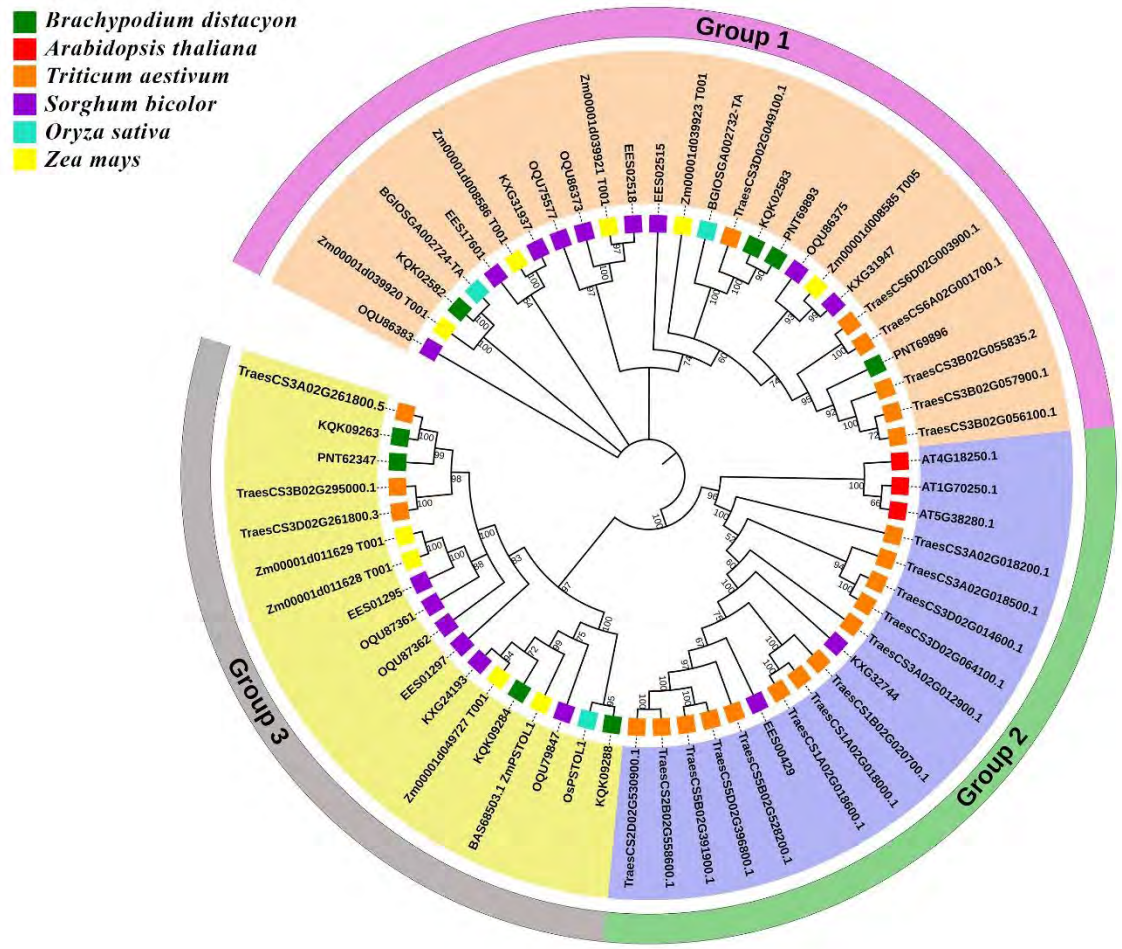

Figure 3.3: *PSTOL1* wheat orthologs in *Triticum aestivum L.* and *Arabidopsis thaliana*, *Sorghum bicolor*, *Zea mays*, and *Oryza sativa*. All 62 orthologs were aligned in CLUSTALW, and a phylogenetic tree was constructed in MEGA 7.0 using the NJ method. Orthologs in different species are shown with other colored squares.

3.4 Duplication Events and Ka\Ks Analysis

To make the map of chromosome distribution, the physical locations of 22 wheat orthologs were taken from GFF3 files, and the map was drawn using TBtools. It is observed that the *TaPSTOL1* were predicted on 11 chromosomes (1A, 1B, 2B, 2D, 3A, 3B, 3D, 5B, 5D, 6A, and 6D) and no orthologs were predicted on other chromosomes (Figure 3.4.1 and 3.4.2).

As wheat is one of the oldest polypoid crops that underwent three hybridization events throughout its evolution. This polyploidization has caused wheat to have over and above 85% repetitive DNA. Because of repetitive DNA, many genes duplicate over time. This duplication event can lead these genes to acquire either neofunctionalization (gene developing new function after particular duplication event), subfunctionalization (paralogs retaining a part of the original gene's functions), or non-functionalization (fate most common after duplication as gene loses all functionality) (Lynch et al., 2001). Hence, it is necessary to study duplication events to understand the functionality and the evolutionary relationship of different duplicated genes.

According to the criteria mentioned in (materials and methods), duplicated genes were identified among 22 wheat *PSTOL1* orthologs. Four of the 22 orthologs were tandem duplicates (duplicate genes present on the same chromosome), and 4 were segmental duplicates (duplicate genes present on different chromosomes). The four segmental duplicates were predicted on chromosomes (2B and 2D), (3A and 3B), (5B and 5D), and (6A and 6D).

Table 3.1: Segmental duplicates within 22 *PSTOL1* wheat orthologs predicted

Tandem Duplicates	
TraesCS1A02G018000	TraesCS1A02G018600
TraesCS3B02G055835	TraesCS3B02G056100
TraesCS3B02G056100	TraesCS3B02G057900
TraesCS5B02G391900	TraesCS5B02G528200

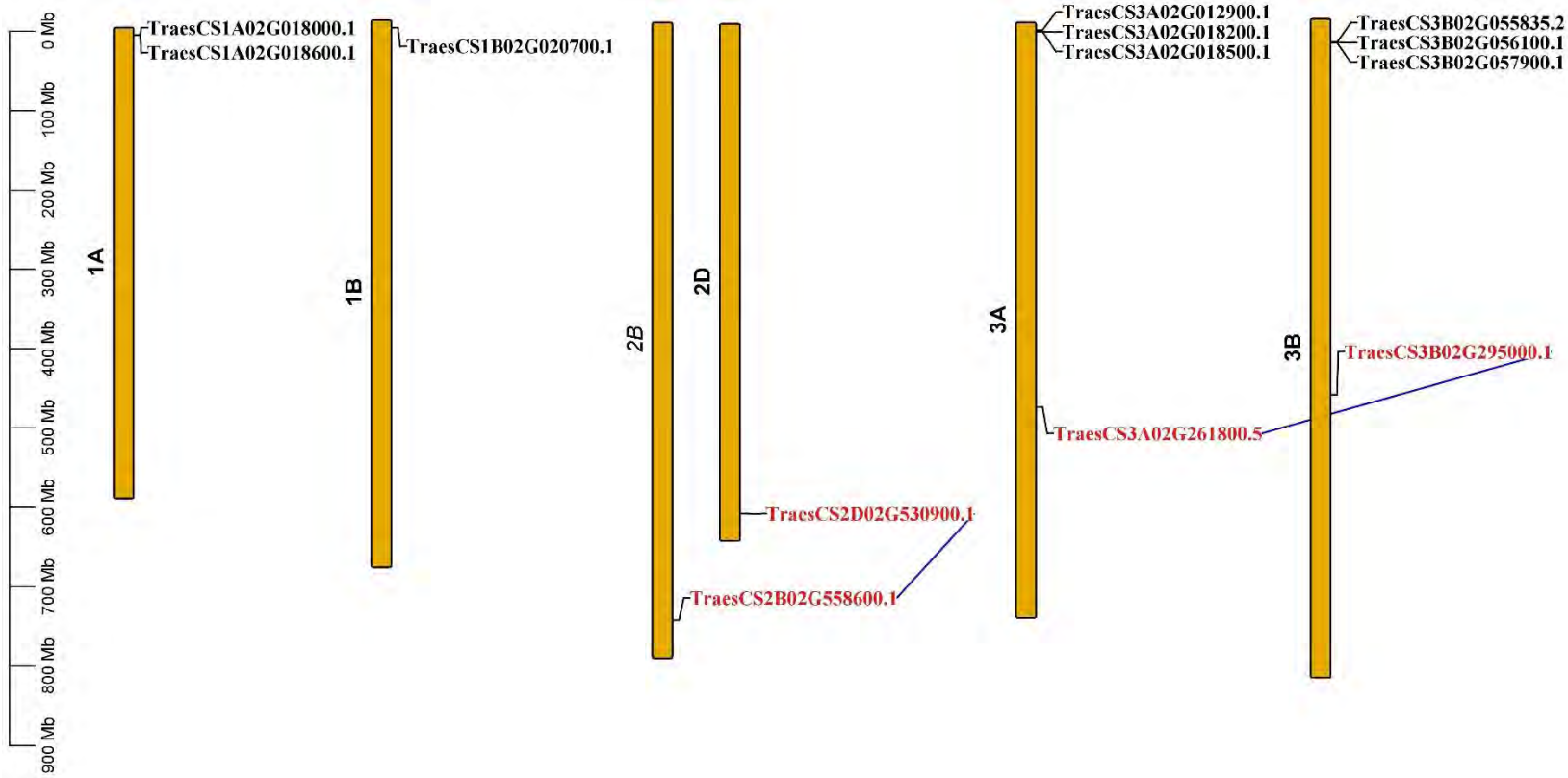

Figure 3.4.1: Chromosomal location and segmental duplicates. 1A, 1B, 2B, 2D, 3A, and 3B represent chromosome numbers. The ruler on the left side indicates chromosome size in megabase pairs (Mbps). Red-colored gene labels show segmental duplicates, and the blue lines indicate a duplicate link.

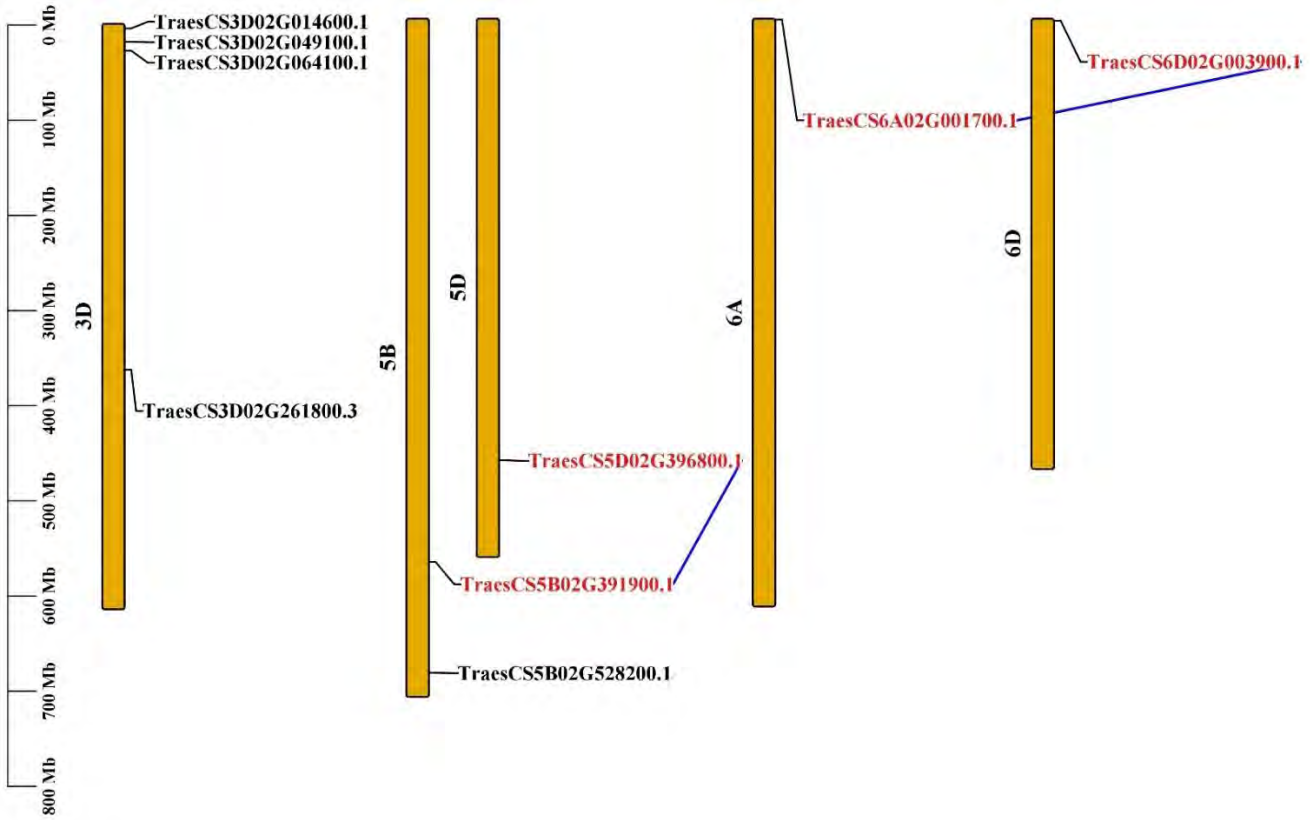

Figure 3.4.2: Chromosomal location and segmental duplicates. 3D, 5B, 5D, 6A, and 6D represent chromosome numbers. The ruler on the left side indicates chromosome size in megabase pairs (Mbps). Red-colored gene labels show segmental duplicates, and the blue lines indicate a duplicate link.

To further understand the evolutionary relationship and selection pressure on the genes, nonsynonymous and synonymous substitution rates (Ka/Ks) were calculated using both tandem and segmental duplicates (Yi-Qin et al., 2020). Ka/Ks <1 indicates purifying or negative selection (selective removal of harmful genes or alleles and leaving specific and essential genes). Ka/Ks =1 implies neutral selection while Ka/Ks >1 indicates positive or natural selection (Darwinian selection in which individual genes are selected by nature on their phenotypic importance). All tandem and segmental duplicates had Ka/Ks <1, implying that these genes underwent strong negative or purifying selection (Table 3.2). With Ka/Ks, the divergence time of these genes was calculated between 3-53 million years ago (Tyagi et al., 2020).

Table 3.2: Ka\Ks ratio and divergence time calculated by KaKs Calculator 2.0

Seq_1	Seq_2	Ka	Ks	Ka/Ks	Divergence Time (MYA)
TraesCS1A02G018600.1	TraesCS1B02G020700.1	0.0283053	0.194875	0.145249	14.990384
TraesCS2B02G558600.1	TraesCS2D02G530900.1	0.0336806	0.101222	0.33274	7.786307
TraesCS3A02G261800.5	TraesCS3D02G261800.3	0.265657	0.466528	0.569434	35.886769
TraesCS5B02G391900.1	TraesCS5D02G396800.1	0.0309779	0.139284	0.222409	10.714153
TraesCS6A02G001700.1	TraesCS6D02G003900.1	0.020903	0.0440992	0.474	3.392246
TraesCS1A02G018000.1	TraesCS1A02G018600.1	0.0762187	0.2352677	0.323966	18.097517
TraesCS3B02G056100.1	TraesCS3B02G057900.1	0.1163265	0.303672	0.383066	23.359385
TraesCS5B02G391900.1	TraesCS5B02G528200.1	0.1873184	0.686024	0.273049	52.771074

3.5 Synteny Analysis of 22 Wheat *PSTOL1* Orthologs with *Aegilops tauschii, Triticum urartu, Triticum dicoccoides,* and *Triticum turgidum*

50-70 million years had passed since the Gramineae family evolved, and about 20 have passes when its sub-family Pooideae evolved. Pooideae sub-family contains barley, wheat, oats, rye, and many more cereal and grass crops (Yi-Qin, H *et al*., 2020). Upon analysis of 22 *PSTOL1* orthologs with ancestors in synteny, we identified 34 self-syntenic gene pairs, 3 gene pairs with *Aegilopes tauschii*, 14 with *Triticum dicoccoides*, 19 with *Triticum turgidum,* and 10 gene pairs were found with *Triticum urartu* (Figure 3.5)

This emphasizes that wheat *PSTOL1* genes were retained more from *T. turgidum*, *T. dicoccoides, T. urartu,* and *Aegilopes tauschii*, respectively. A and B sub-genomes of hexaploid wheat had fewer *PSTOL1* genes than wheat progenitors. This indicates that some *PSTOL1* genes might have been lost during polyploidization. At the same time, the D sub-genome showed an increased gene number in hexaploid wheat. This indicates that copy number increases during wheat polyploidization events.

3.6 Expression Patterns of Wheat *PSTOL1* Orthologs in Transcriptomic Data

The data collected from contained TPM values. TPM value data was collected of roots and shoots at the vegetative stage in both control and phosphorus stressed plants. The collected data was used to create a heatmap in TBTools (Figure 3.6) from which it is evident that TraesCS3A02G261800.5 gene was downregulated in both roots and shoots under phosphorus stress plants while up-regulated in control plant roots and shoots. Contrary to this, TraesCS3A02G018500.1 was found to be highly upregulated in both treated roots and shoots and downregulated in control roots and shoots. Also, TraesCS3B02G295000.1 was up-regulated in control conditions while downregulated in stress conditions. TraesCS5B02G391900.1 and TraesCS5D02G396800.1 also upregulated in roots and shoots treated with phosphorus deficient conditions while down regulated in control tissues.

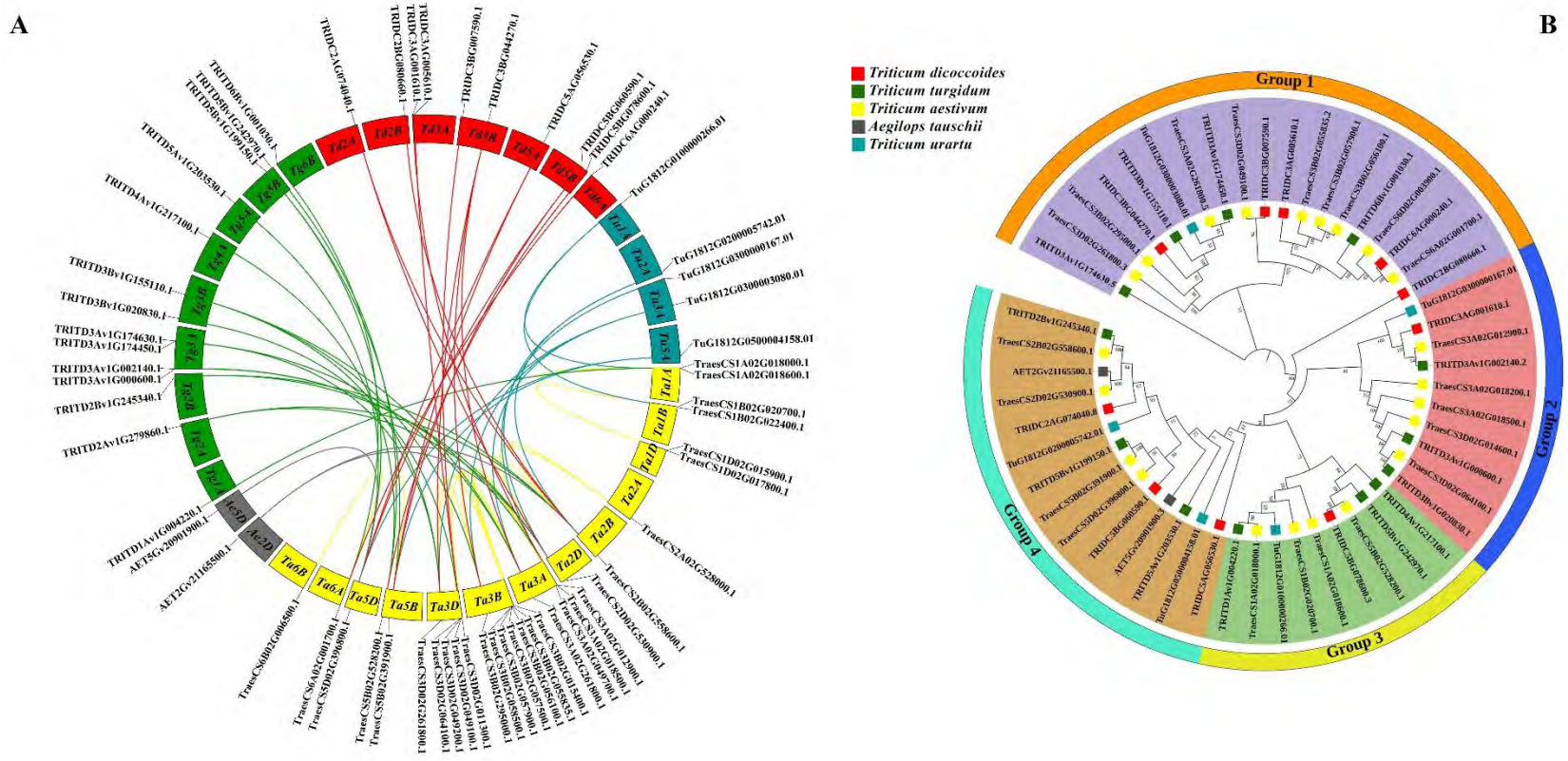

Figure 3.5: Syntenic and evolutionary analysis of *PSTOL1* wheat orthologs with ancestral species. **(A)** Synteny analysis; **(B)** Phylogenetic tree of 22 Triticum aestivum L. *PSTOL1* orthologs with *Aegilops tauschii*, *Triticum urartu*, *Triticum dicoccoides*, and *Triticum turgidum*. Red-colored rectangles represent Triticum dicoccoides, green for *Triticum* turgidum, gray for *Aegilops tauschii*, blue for *Triticum urartu*, and yellow for *Triticum aestivum* L

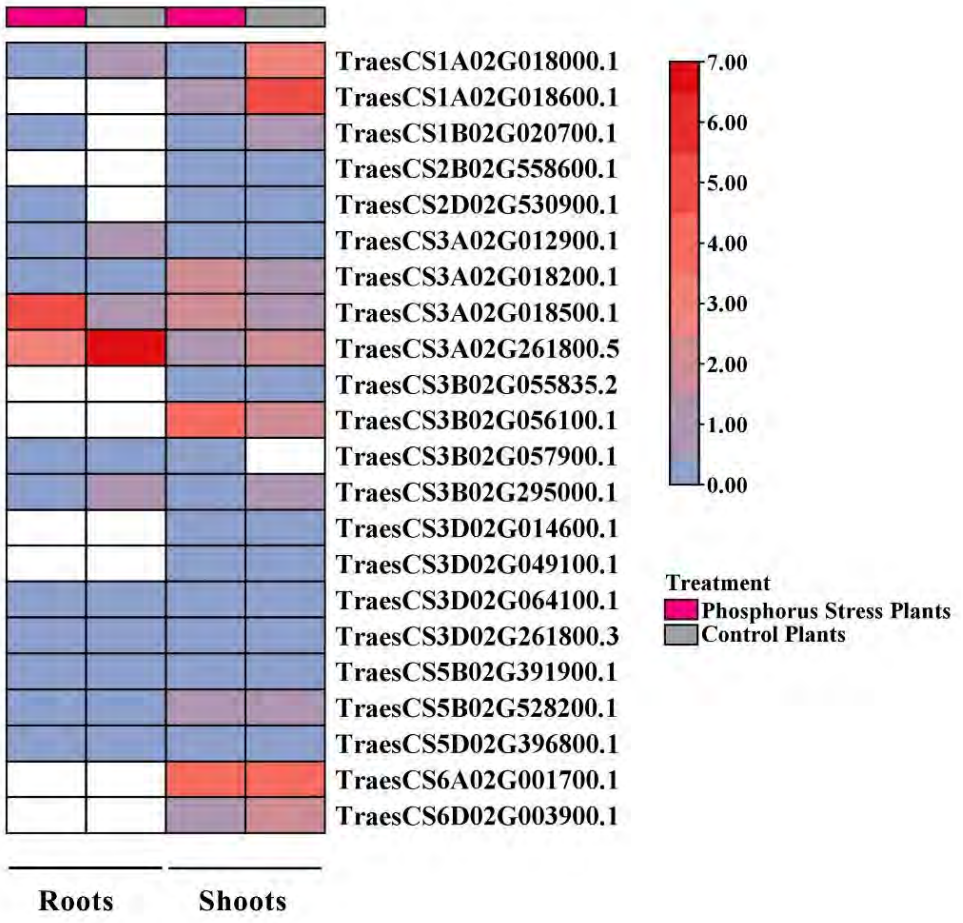

Figure 3.6: Gene expression profiling of *TaPSTOL1* gene in root and shoot tissues under normal and phosphorus-deficient treatment conditions. Expression data was acquired from the wheat expression browser in the TPM values and presented in the form heatmap. Color patterns illustrate the down and up-regulated genes.

3.7 Morphological Evaluation under Phosphorus Sufficient and Deficient Conditions

By visualizing the plants (Figure 3.7.1), shoots of both plant genotypes under phosphorus stress showed limited and stunted growth. Pak-13 showed better shoot growth in phosphorus-sufficient conditions than tap water, while Shafaq-06 plant shoots were less affected in both conditions.

Figure 3.7.1: Plants' response towards control and P starvation condition. On top are the Pakistan-13 plants, showing comparison between plants under -P, C and +P conditions. Similarly, the bottom image shows Shafaq-06 plants, showing comparison between plants under -P, C and +P conditions.

Morphological data showed that the shoot length of Shafaq-06 under control condition was approximate 21-32 cm with an overall mean of 27.93cm, for phosphorus sufficient plants, the range was about 28-35 cm with the mean of 31.60cm while for plants treated with phosphorus deficiency showed range 29-36 cm with the average of 31.40cm.

In the case of Pakistan-13, the shoot length for control plants was observed to be in the range of 36-31cm with the mean of 29.53cm, for phosphorus sufficient plants, the mean was 33.63cm with the range between 32-35 cm, and for phosphorus-deficient plants, the range was between 25-30cm with an overall mean of 27.57cm (Figure 3.7.2). The result of ANOVA showed $p > 0.05$. Hence, the LSD All-Pairwise Comparison Test showed no significant pairwise differences between the means for either genotype, treatment, or genotypes x treatment. Moving towards the tiller count of the plants, both genotypes showed similar results with an average of 3 tillers per plant for phosphorus sufficiency treatment, while 2 tillers per plant in case of both control and phosphorus-deficient conditions (Figure 3.7.3). ANOVA showed a $p > 0.05$; hence the LSD All-Pairwise Comparison Test showed no significant pairwise differences between the means for either genotype, treatment, or genotypes x treatment.

The fresh shoot weight under control conditions showed the range of 0.4-4g (Shafaq-06) and 2.1-2.3g (Pak-13), with an overall mean of 2.2g for both. Under phosphorus sufficient conditions, Shafaq-06 plants were in the range of 3-3.6g while Pakistan-13 plants were between 2.5-4g with an average of 3.26g and 3.22g each. Lastly, in phosphorus-deficient conditions, Shafaq-06 plants showed 1-3g while Pakistan-13 showed a range of 1-2g with the overall means of 2.15g and 1.9g (Figure 3.7.4). ANOVA showed the $p > 0.05$ and showed no significant difference among the mean values. Still, the LSD All-Pairwise Comparison Test for treatment showed that means of +P and -P are divided into 2 different groups with significantly different means among them. Under control conditions, the dry shoot weights were in the range of 0.05-0.5g (Shafaq-06) and 0.35-0.4g (Pak-13), with an overall mean of 0.33g and 0.38g. Under +P conditions, both Shafaq-06 and Pak-13 plants exhibited the range of dry shoot weight to be 0.4-0.6g with averages of 0.49g and 0.5g. In phosphorus-deficient conditions, both Shafaq-06 and Pak-13 plants were in the range of 0.2-0.5g with overall means of 0.35g and 0.38g (Figure 3.7.5). ANOVA showed $p > 0.05$, and along with LSD All-Pairwise Comparison Test, there was no significant difference between the means.

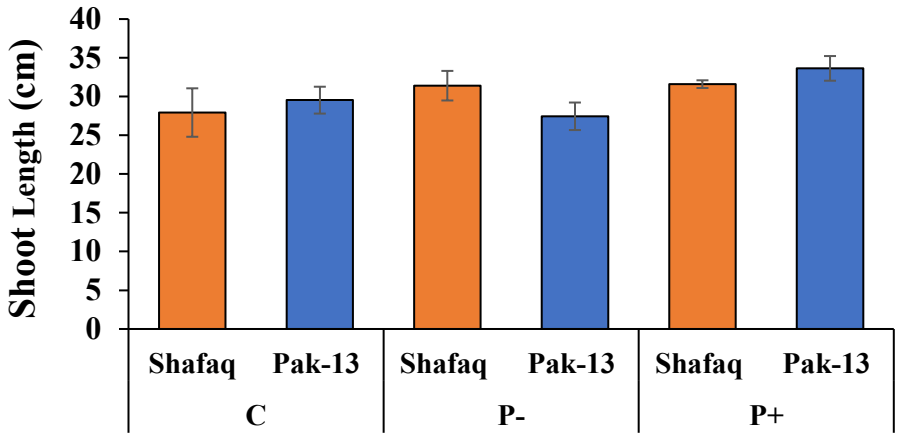

Figure 3.7.2: Shoot length of both genotypes under control and treated conditions

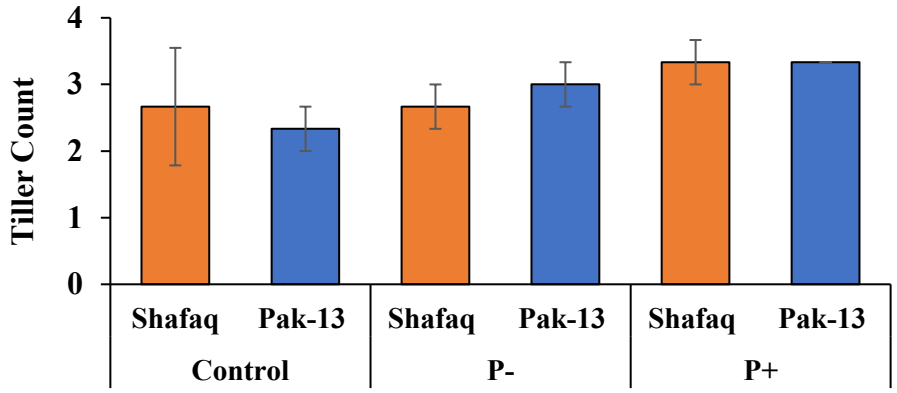

Figure 3.7.3: Tiller count of both genotypes under control and treated conditions

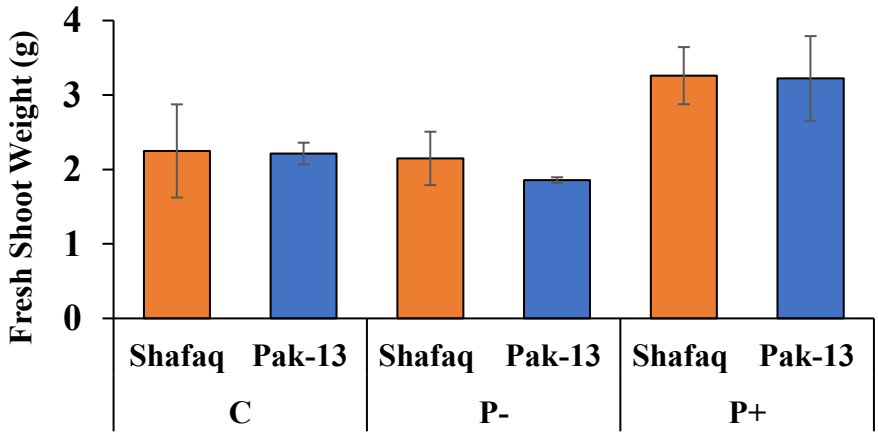

Figure 3.7.4: Fresh shoot weight of both genotypes under control and treated conditions

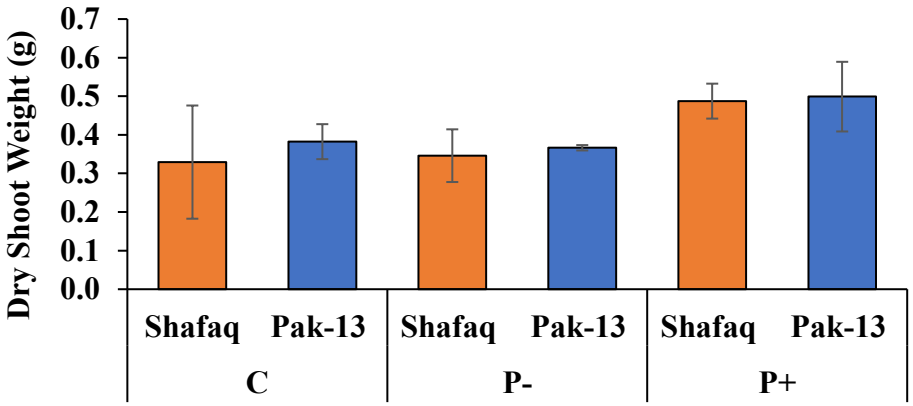

Figure 3.7.5: Dry shoot weight of both genotypes under control and treated conditions

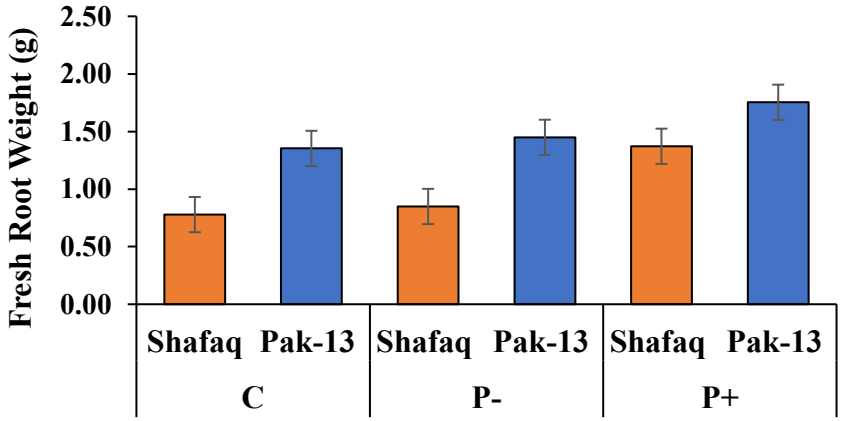

Figure 3.7.6: Fresh root weight of both genotypes under control and treated conditions

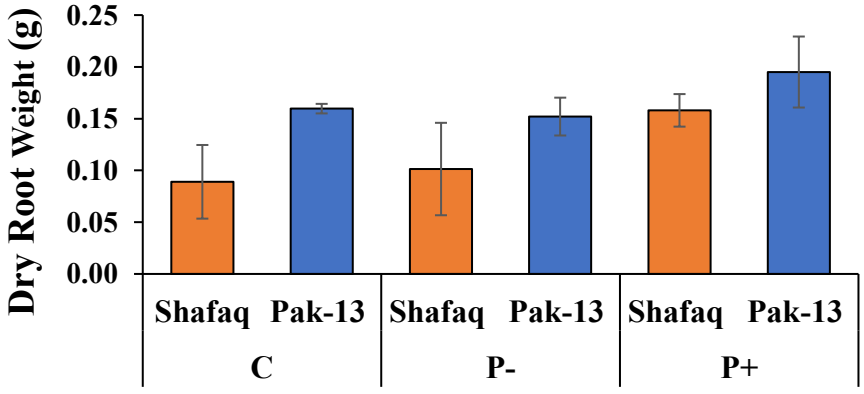

Figure 3.7.7: Dry root weight of both genotypes under control and treated conditions

Fresh root weight was taken after cautiously washing off all the debris on plant roots. The fresh root weight under control conditions of Shafaq-06 plants was in the range of 0.1-1.3g with a mean of 0.78g. Pak-13 plants were in between 1.1-1.6g with an overall mean of 1.35g. Under +P conditions, Shafaq-06 plants were in the range of 1.2-1.5g with an average value of 1.37g, while Pak-13 plants showed the mean value of 1.75g with the range of 1.4-2.1g. Similarly, under -P conditions, the Shafaq-06 plants were in the range of 0.3-2g with an average of 0.85g, while Pak-13 plants were in the range of 1.1-1.8g with the mean value of 1.39g (Figure 3.7.6). ANOVA showed the $p < 0.05$ (0.02) for genotypes. With the LSD All-Pairwise Comparison Test, the genotypes were divided into 2 groups, indicating that the means of both genotypes for fresh root weight were significantly different from each other. Also, in the case of genotype x treatment, the means were divided into 2 groups showing both groups were significantly different from each other.

For root dry weight under control conditions, Shafaq-06 plants were in the range of 0.01-0.4g with an average of 0.09g, while Pak-13 plants were in the range of 0.1-0.2g with the mean of 0.16g. In +P conditions, Shafaq-06 plants were in the range of 0.15-0.17g with the average value of 0.16g, while Pak-13 plants with the mean value of 0.20g were in the range of 0.1-0.22g. In -P condition, Shafaq-06 plants were in the range of 0.04-0.19g with an average value of 0.10g, and Pak-13 plants were in the range of 0.1-0.17g with an overall mean of 0.16g (Figure 3.7.7). ANOVA showed $p < 0.05$ (0.03) for genotypes, along with LSD All-Pairwise Comparison Test, it was clear that both genotypes had a significant difference among their means. Also, in the case of genotype x treatment, the means were divided into 2 groups showing both groups were significantly different from each other.

3.8 Physiological Parameters Analysis

Upon calculating chlorophyll content, it was observed that under control conditions, Shafaq-06 plants had chlorophyll content in the range of 1000-1800 ug/g with an average of 1381 ug/g, while Pak-13 plants had 1000-1700 ug/g with mean of 1342 ug/g. In +P conditions, Shafaq-06 plants ranged between 800-850 ug/g with an average of 831 ug/g, while Pak-13 plants had 1342 ug/g with the range of 1000-1700 ug/g. In -P condition, Shafaq-06 plants had mean chlorophyll content of 197.72 ug/g with the range between 190-

230 ug/g, while Pak-13 plants contained about 156.90 ug/g chlorophyll content on average with the range of 150-160 ug/g (Figure 3.8.1). ANOVA resulted in $p \leq 0.001$, showing a highly significant difference between the means in treatment comparison. According to LSD All-Pairwise Comparison Test, the -P treated plants were placed in group B while control and +P plants were in group A showing both of their means were not significantly different. NDVI measurement in Shafaq-06 plants showed a high value of 0.31 in -P conditions compared to both control and phosphorus sufficient conditions (0.27 and 0.29). Similarly, Pak-13 plants showed 0.44 in phosphorus deficient conditions compared to both control and +P conditions (0.26 and 0.32) (Figure 3.8.2). Both NDVI and chlorophyll content values coincide, depicting that the plants with more chlorophyll content had higher NDVI values.

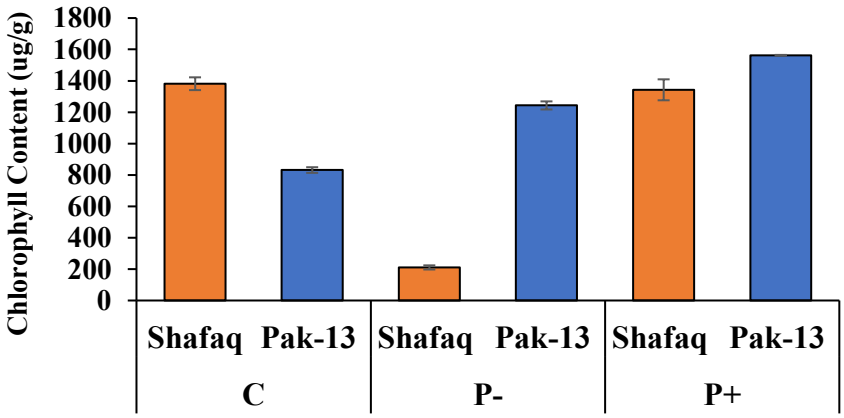

Figure 3.8.1: Chlorophyll content of both genotypes under control and treated conditions

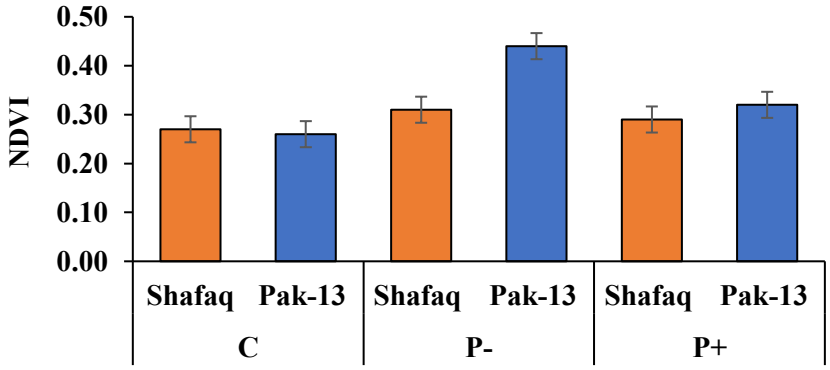

Figure 3.8.2: NDVI values of both genotypes under control and treated conditions

3.9 Bio-physiochemical Parameters Analysis

Phosphorus content was measured in both shoots and roots of all replicates for both genotypes. Roots of Shafaq-06 in both control and +P conditions showed uptake of (0.43% and 0.44%), while in the -P condition, the phosphorus uptake (0.38%) was slightly less in comparison. In Pak-13 roots, the phosphorus content was higher in both phosphorus sufficient and deficient conditions (0.44% and (0.41%) while slightly less in the control (0.38%) condition (Figure 3.9). In the case of shoots, the phosphorus accumulated excessively in +P conditions for both genotypes with Pak-13 showing the highest value (1.16%) with Shafaq-06 showing (1.07%). Under control conditions phosphorus content was 0.57% in Shafaq-06 plant roots and 0.73% in Pak-13 roots. In phosphorus-deficient conditions Shafaq-06 shoots accumulated less (0.82%) than Pak-13 (0.87%). This shows that Pak-13 was responding to change by trying to mine more phosphorus than Shafaq-06 plants in phosphorus-deficient conditions (Figure 3.9)

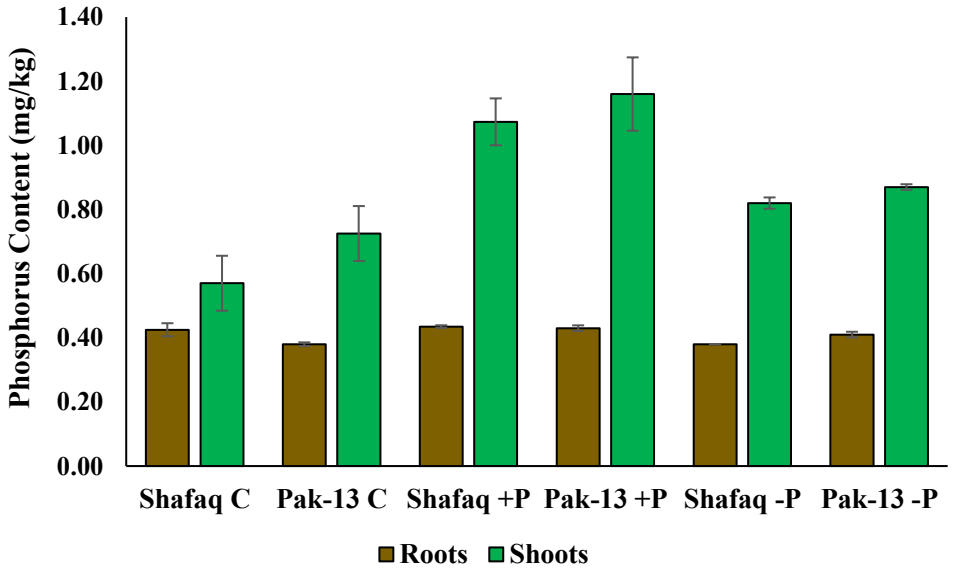

Figure 3.9: Phosphorus content in shoots and roots of Shafaq-06 and Pak-13, under control, phosphorus sufficient, and deficient conditions.

For the roots, ANOVA showed that the means of phosphorus content were highly significantly different ($p \leq 0.01$) from one another in case of treatment. For genotype and treatment x genotype, the means showed significant differences ($p < 0.05$).

In the case of phosphorus content in shoots, the difference in the means was found to be highly significant ($p \leq 0.01$) for treatment, while the results were non-significant ($p > 0.05$) for both genotype and treatment x genotype.

3.10 High-Throughput Root Phenotyping Analysis

Roots were scanned and analyzed under RhizoVision (Figure 3.10.3). The root length (RL), the average diameter (AD), volume (V), and surface area (SA) were calculated using RhizoVision. Compared to control and phosphorus sufficient conditions, the (RL) root length for Pak-13 increased under phosphorus deficient conditions. Contrary to this, Shafaq-06 showed an increase in root length under phosphorus-sufficient conditions and remained similar in both control and phosphorus-deficient conditions. Under control conditions, the root length for Pak-13 lay in the range of 3330-3800 mm, while Shafaq-06 lay in 2600-3500 mm. In phosphorus sufficient conditions Pak-13 showed the range of 2800-3100 mm while Shafaq-06 was 3300-3900 mm. In phosphorus-deficient conditions, Pak-13 root length lay in the range of 3500-3900 mm, while for Shafaq-06, the range was between 2900-3100 mm (Figure 3.10.1).

With the mean value of 10924 $mm^{3,}$ the root volume was seen to increase drastically in Pak-13 as compared to Shafaq-06 (6429 mm^3) under phosphorus-deficient conditions. In control conditions, Shafaq-06 showed quite an increase in root volume (13590 mm^3) compared to Pak-13 (5817 mm^3). In phosphorus sufficient conditions, a slight increase was observed in the root volume of Shafaq-06 (7814 mm3) compared to Pak-13 (5817 mm^3) (Figure 3.10.1). The surface area of roots was observed to be in correspondence with root volume. Most of the plants that showed higher root volume also had a higher surface area and vice versa. In phosphorus-deficient conditions, the surface area was more elevated in Pak-13 (15512 mm^2) than Shafaq-06 (10022 mm^2). While in control conditions surface area of roots was higher (17324 mm^2) in Shafaq-06 as compared to Pak-13 (11224 mm^2) (Figure 3.10.1).

For average diameter (AD), Pak-13 with the mean value of 0.89 mm showed decrease in -P conditions. In Shafaq-06, the average root diameter with mean values of 1.5mm and 1.4mm, did not significantly differ in +P and -P. The diameter was 1.3 mm in Pak-13 and 2.7 mm in Shafaq-06 under control conditions (Figure 3.10.2). The range of root diameter in +P condition was recorded to be 1.1-1.25 mm in Pak-13 and 1.2-2 mm in Shafaq-06. In -P conditions, the range was 0.7-1.2 mm in Pak-13 while 1.3-1.7 mm in Shafaq-06. Finally, in the control condition, the range was recorded as 1-1.5 mm in Pak-13 and 2.1-4 mm in Shafaq-06.

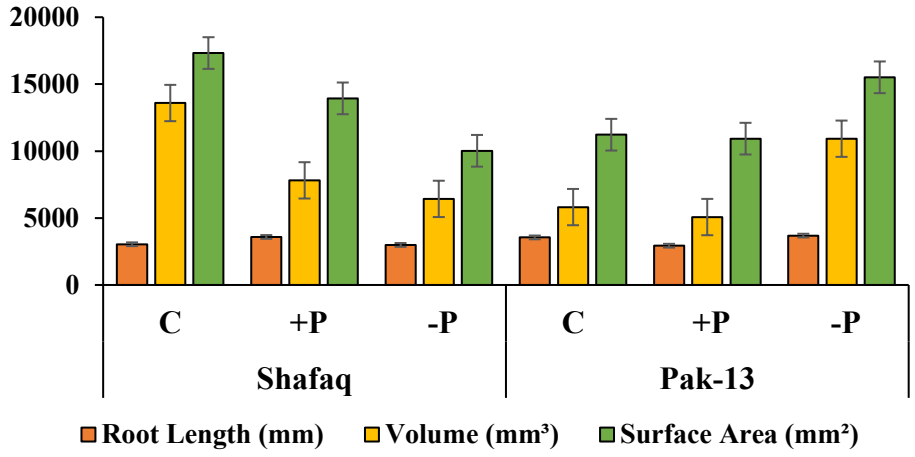

Figure 3.10.1: Bar graph showing root length, volume, and surface area of roots among Pakistan-13 and Shafaq-06 varieties under control, +P and -P conditions.

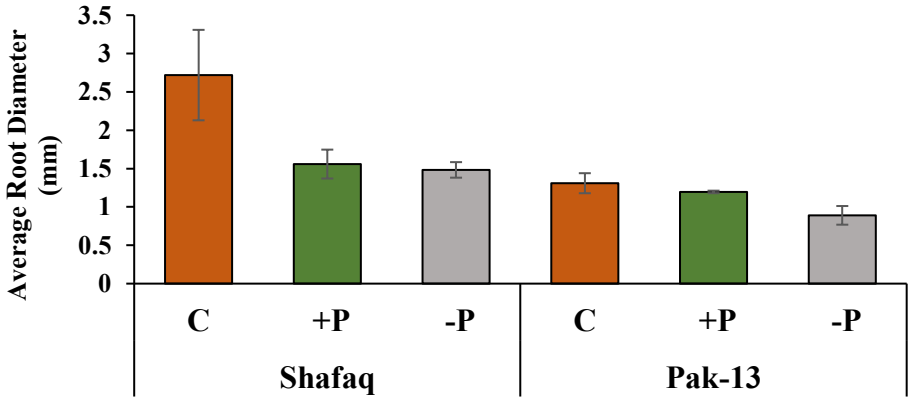

Figure 3.10.2: Bar graph representing root diameter in Pakistan-13 and Shafaq-06 varieties under control, +P and -P conditions.

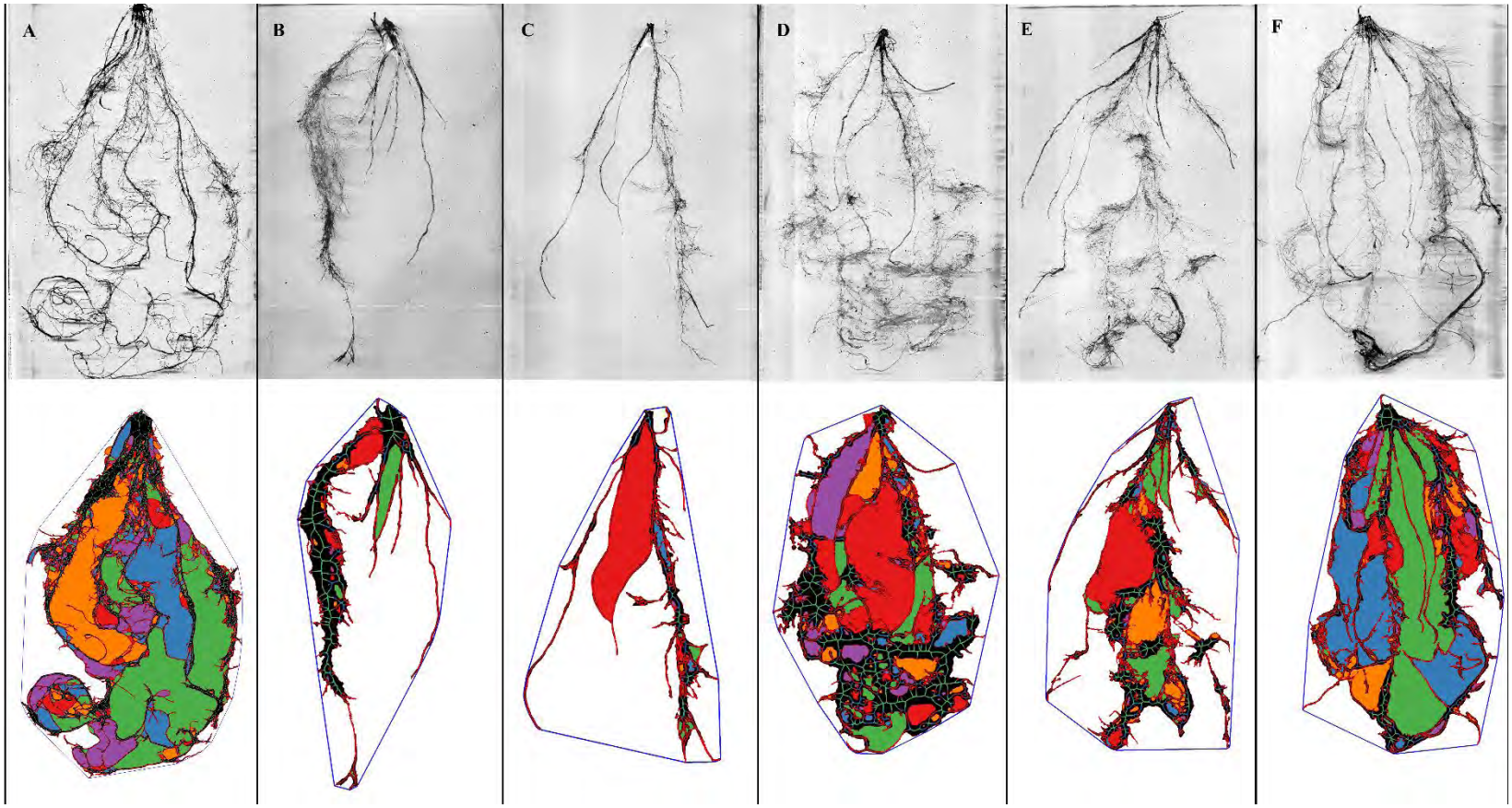

Figure 3.10.3: Root images analyzed in RhizoVision Explorer. (**A**) Shafaq-06 +P plant root with root analyzed image (**B**) Shafaq-06 -P plant root scanned and analyzed image (**C**) Shafaq-06 C plant root scanned and analyzed image (**D**) Pak-13 +P plant root scanned and analyzed image (**E**) Pak-13 plant -P plant root scanned and analyzed image (**F**) Pak-13 plant C plant root scanned and analyzed image.

The analysis of variance (ANOVA) of the root lengths obtained from RhizoVision Explorer software showed that the means were significantly different from each other. Results were significant in the case of genotype ($p < 0.05$) while it was highly significant in the case of genotype x treatment ($p < 0.01$). The result for root length was not significant in the case of treatment ($p > 0.05$). Upon further applying the LSD all-pairwise comparison test, the means were divided into 2 groups (A and B) for genotype and treatment x genotype.

In the case of root volume, the result of ANOVA showed that the means of all plants showed a highly significant difference ($p < 0.01$) in the case of treatment, treatment x genotype, and ($p \leq 0.01$) in genotype. Based on the LSD test, the mean for C and -P was placed in 1 group (A). The mean of (+P) was placed in the 2nd group (B). Similarly, the LSD test put both genotypes into different groups and divided the means into 4 other groups for treatment x genotype interaction.

The result was highly significant ($p < 0.01$) for root surface area in the case of treatment x genotype. ANOVA results for both genotype and treatment were non-significant ($p > 0.05$). LSD test divided the means into 3 groups treatment x genotype interaction while keeping means in 1 group for both treatment and genotype. For diameter, the ANOVA result showed a significant difference ($p < 0.05$) for treatment interactions while showed a highly significant difference ($p < 0.01$) between means in the case of genotypic interactions. The results showed non-significant difference ($p > 0.05$) for treatment x genotype interaction.

3.11 Correlation of Morphological Traits

The correlation of morphological traits was performed in R, using "correlate" and "agricolae." The analysis revealed that the plant root length (RL) had a positive correlation with NDVI, dry root weight (DRW), dry shoot weight (DSW), root volume (RV), and root surface area (RSA). RL showed a negative correlation with chlorophyll content (CC), fresh shoot weight (FSW), tillers, root diameter (RDM), and shoot length (SL). All of the correlations of (RL) showed non-significant difference ($p > 0.05$). Shoot length (SL), tillers, FSW, DSW, FRW, DRW and CC, root phosphorus content (RPC), and shoot phosphorus content (SPC) all showed a positive association with each other. The maximum

correlation was found between FRW and DRW. These 8 parameters showed a negative correlation with RDM, RV, and RSA (Figure 3.11). A significant difference ($p < 0.05$) was found between SL and RV, tillers and DSW, DRW and DSW, and SPC and tillers. A highly significant difference ($p < 0.01$) was observed between tillers and FSW, FSW and DSW, RV and RSA, SPC and DSW, and SPC and DRW.

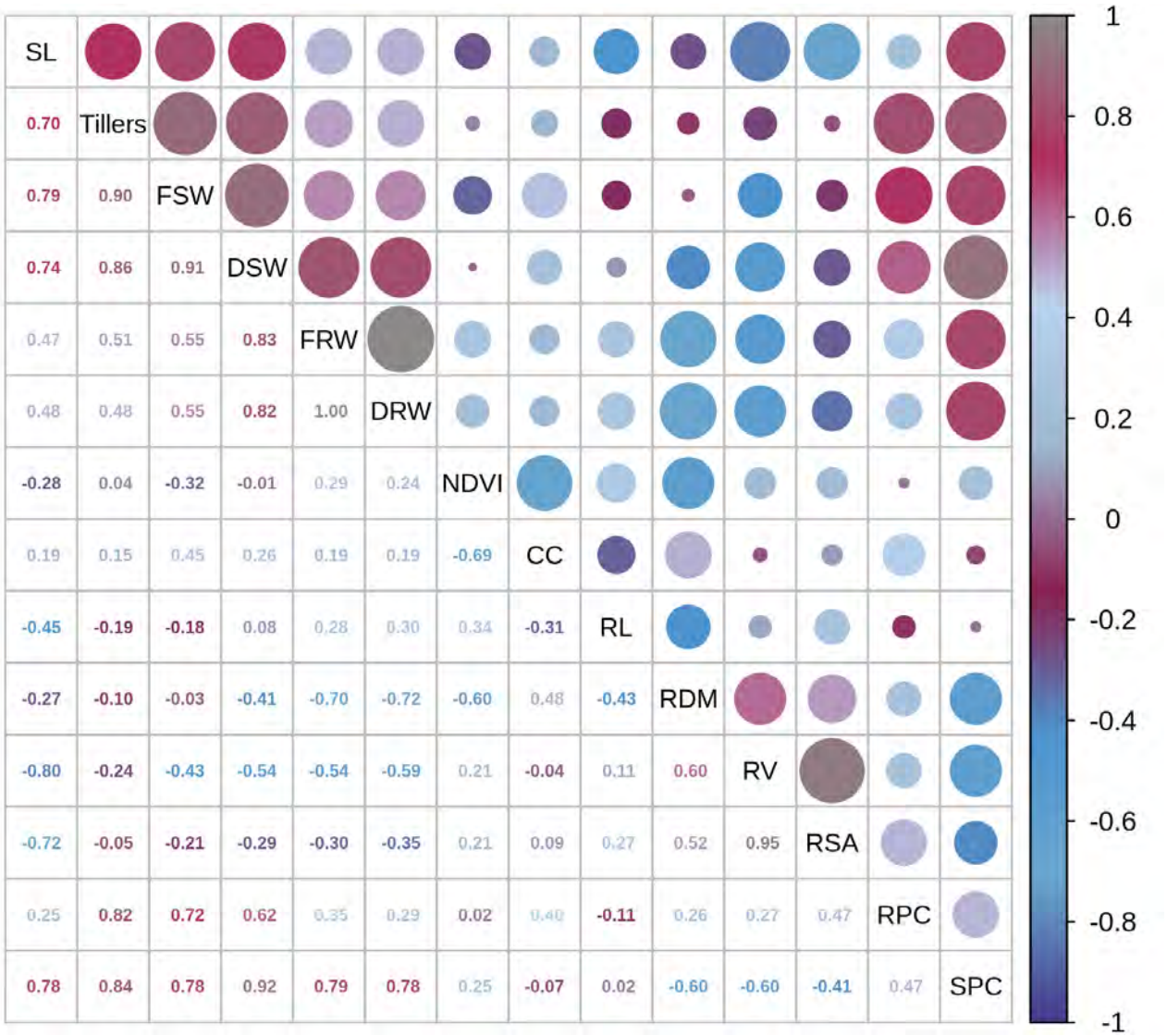

Figure 3.11: Correlation between all morphological, physiological, and bio-physiochemical traits. Correlation values are shown below the diagonal. Above the diagonal the size and color of circles represent the correlation intensity. Ruler on right side indicates positive and negative correlation.

3.12 RNA Extraction and Expression Analysis

Total RNA was extracted from roots of Shafaq-06 and Pak-13 plants under control, phosphorus sufficient, and deficient conditions. Extracted RNA was visualized using Gel Electrophoresis and a gel documentation system (Figure 3.12.1).

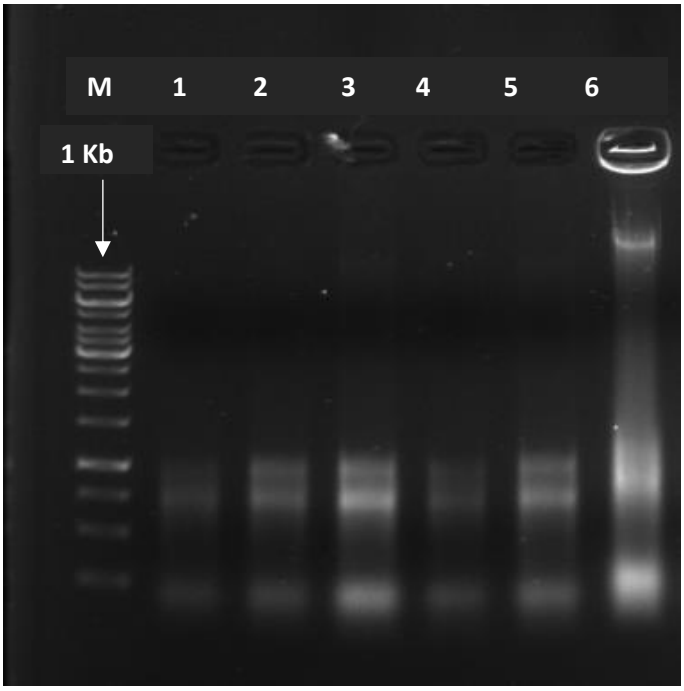

Figure 3.12.1: Extracted RNA from roots of Shafaq-06 and Pak-13 plants under C, +P, and -P conditions. 1 and 2 wells contain RNA of Shafaq-06 and Pak-13 under +P conditions, 3 and 4 wells contain RNA of Shafaq-06 and Pak-13 under -P conditions while 5 and 6 wells contain RNA of Shafaq-06 and Pak-13 under C conditions.

Extracted RNA was used to create cDNA and perform expression analysis of selected genes on RT-PCR. For gene TraesCS3A02G018500.1 the relative expression in Shafaq-06 plants was highest under phosphorus sufficient condition, lower in -P condition, and least in the control condition. In comparison, this gene was highly expressed in phosphorus-deficient condition for Pak-13, lower in the control condition and least in phosphorus sufficient condition. There was a highly significant difference ($p < 0.01$) between the means of relative expression under control and phosphorus-deficient conditions in Pak-13 and between +P and phosphorus deficiency. There was a significant difference ($p < 0.05$) between phosphorus deficiency and +P condition for Pak-13.

Expression of gene TraesCS3A02G018500.1 was up-regulated under phosphorus deficiency in the data obtained from wheat expression browser, and Pak-13 plants responded similarly in our study. Pak-13 plants showed upregulation of this gene under phosphorus deficiency, while Shafaq-06 plants showed the opposite result by expressing this gene more in phosphorus-sufficient conditions. This indicates that this gene could be the wheat *PSTOL1* ortholog (Figure 3.12.2 - A).

In the wheat expression browser, TraesCS3B02G295000 was downregulated under phosphorus-deficient conditions and was up-regulated in control conditions. Our study showed the opposite result in both varieties with upregulation of this gene in phosphorus-deficient conditions. There was a slight expression in phosphorus-sufficient conditions for Pak-13 plants, while Shafaq-06 showed almost similar expression in both control and phosphorus deficient conditions. In Pak-13, there was a highly significant difference ($p < 0.001$) in expression between +P and phosphorus-deficient condition while the rest of the differences were non-significant (Figure 3.12.2 - B).

TraesCS5B02G391900 was up-regulated in phosphorus-deficient conditions and downregulated in a control condition in the expression browser. Similarly, in our study, the expression data revealed that the gene showed higher expression in phosphorus-deficient conditions than control in both genotypes. At the same time, there was an excessive increase in relative expression in phosphorus sufficient conditions for both varieties. In Shafaq-06 plants, there was a significant difference ($p < 0.05$) of expression between phosphorus adequate and deficient conditions. The was a similar case in Pak-13, but the difference was highly significant ($p < 0.01$) (Figure 3.12.2 - C).

TraesCS5D02G396800 was found to be up-regulated under phosphorus-deficient conditions and downregulated in the control condition. In our study, the expression data revealed that in Pak-13 and Shafaq-06, the gene was up-regulated in phosphorus-deficient conditions while downregulating in control conditions.

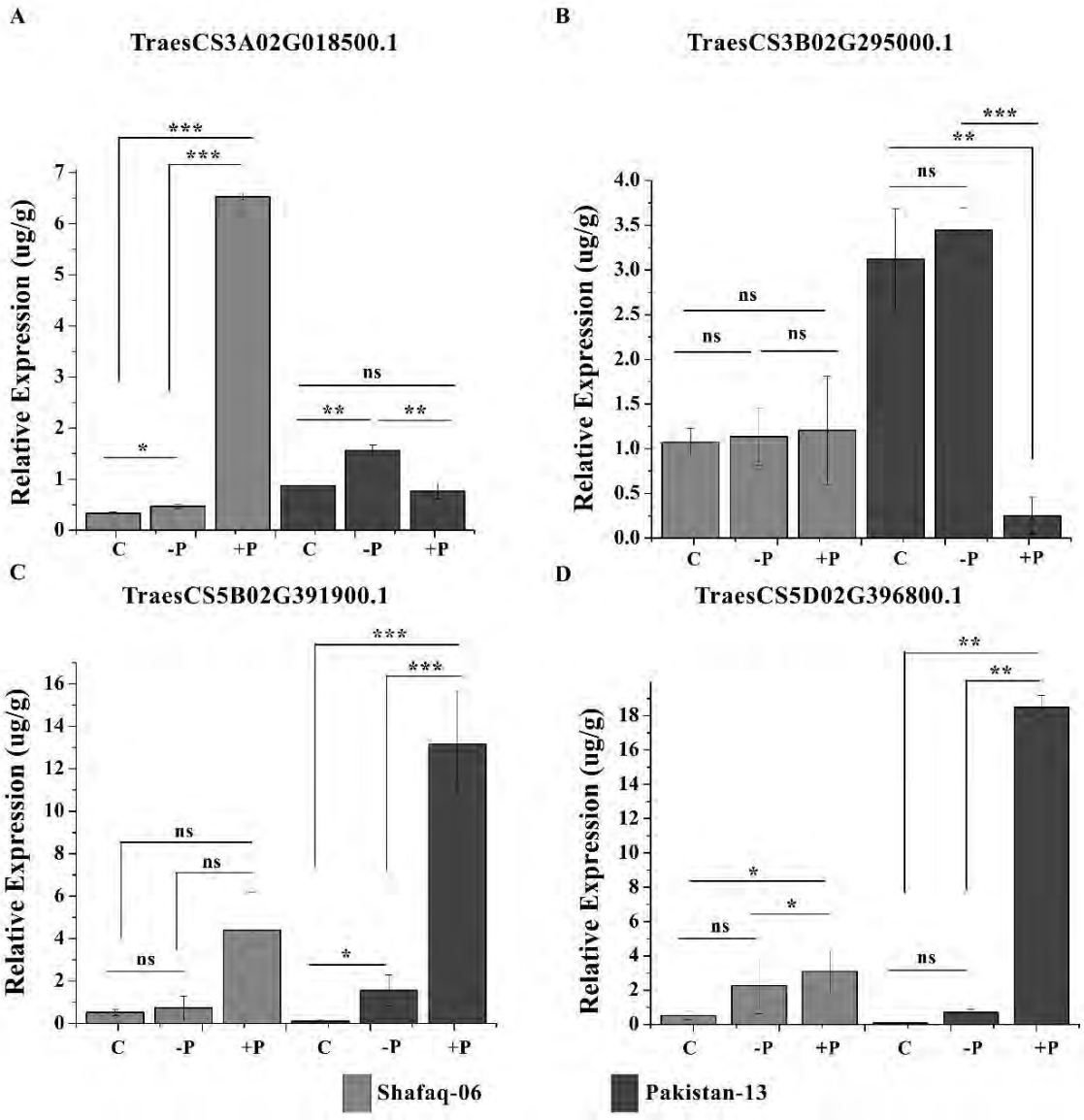

Figure 3.12.2: Relative expression (ug/g) of four genes under phosphorus deficient and control conditions. Asterisks on bars indicate significant difference determined by *T.test* with $p < 0.05$ (*), $p < 0.01$ (**), and $p < 0.001$ (***).

Upon phosphorus sufficient conditions, the gene was excessively up-regulated in Pak-13 and slightly up-regulated in Shafaq-06. In Pak-13 there was significant difference ($p < 0.05$) of expression between control and phosphorus-deficient condition while high significant difference ($p < 0.001$) between +P and phosphorus-deficient condition (Figure 3.12.2 - D).

3.13 Co-localization of *TaPSTOL1* Orthologs with Phosphorus Deficiency Responsive QTLs

To further understand and validate the function of *TaPSTOL1* genes, these orthologs were plotted against reported QTLs. These QTLs were identified for their involvement in maximum root length (MRL), root dry weight (RDW), shoot, root, and total phosphorus content (SPC, RPC, TPC), root diameter (RDM), root tip numbers (RTN), number of axial root length (RN) under phosphorus-deficient conditions. All 22 genes were mapped against QTLs on 10 different chromosomes, i.e., 347 1A, 1B, 2B, 3A, 3B, 3D, 5B, 5D, 6A, and 6D. But only 6 genes were found to be co-localized with the QTLs. Five genes were on chromosome 1A and 3A, while the one gene was on chromosome 2B. TraesCS1A02G018000 and TraesCS1A02G018600 were located within QRdw-1A.2. TraesCS3A02G012900, TraesCS3A02G018200, TraesCS3A02G018500 were in close proximity of QRDW.caas-3AS. In B sub genome, TraesCS2B02G558600 was linked with QRDM.sicau-2B.5 (Figure 3.13).

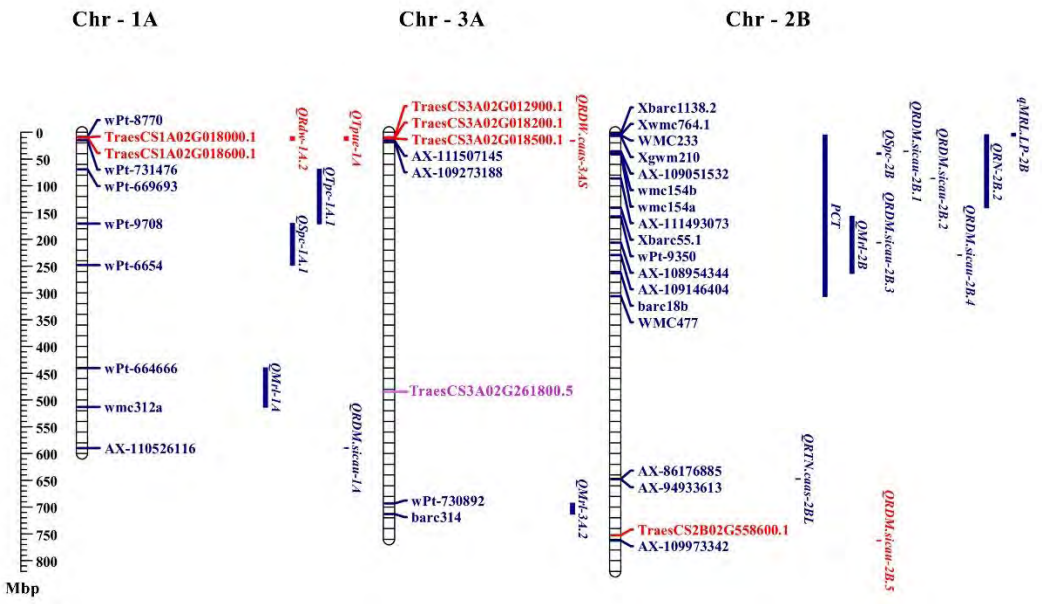

Figure 3.13: Co-localization of 6 *TaPSTOL1* orthologs on three chromosomes, i.e., 1A, 3A, and 2B. Scale on the left-hand side shows the physical position of these genes in Mbp. Genes located within or close to QTLs are illustrated with red color. Genes and QTLs not linked are represented with pink and blue colors.

DISCUSSION

Abiotic stresses are one of the major limiting factors for plant growth worldwide. Research and studies are being conducted around the globe to identify the mechanisms of plants against stress, but producing lines that are tolerant and resistant genomic background behind all these processes are still not clear and completely identified (Vigueira et al., 2016). Phosphorus stress is one such factor that excessively increases farmers' costs because it has to be applied in the form of expensive fertilizers (Azevedo et al., 2015). Plants are trying to survive in phosphorus deficiency by increasing P uptake by modifying their root systems, changing rhizospheres and interacting with microorganisms, or working around with the transport of internal phosphorus and mobilization (Azevedo et al., 2015). Over time, multiple genes have been identified in many different plants that play an influential role in regulating plants' responses to many of these stresses.

With all the tools and genomes available at our disposal, identifying genetic variants of many genes, even in very complex genomes like wheat, has become easier. With the emergence of many bioinformatics tools, studying and understanding comparative genomics is now convenient and effortless (Song et al., 2021). Studying different genes, their functions, structures and performing multiple genome-wide analyses have become fast and convenient. After the release of the first-ever sequenced genome of *Arabidopsis thaliana* in 2000, more than 500 plant genomes have been sequenced. With the increasing amount of genomics and proteomics data available, it has become easier to analyze and study the evolution and evolvement of plant genes. With further advancement in comparative genomics, information from one species can be used to study related species, and many functional variants in species can be identified. Thus, consequences and effects of different genetic variants can be determined because these variants at phylogenetically conserved and variable sites contribute toward different phenotypic variations (Kono et al., 2018).

PSTOL1 gene, which belongs to the RLK family (Lehti-Shiu et al., 2009), is one such variant. Receptor-like kinases (RLK) are involved in controlling growth and defense in plants. It has been found that the expansion of this gene family is significant for the plants to acquire specific adaptations and survive. The main reason for the increase of the RLK gene family is mainly tandem duplication events, and this duplication is

further correlated with stress responsiveness (Lehti-Shiu et al., 2009). *OsPSTOL1* genes were identified upon sequencing of PuP1 QTL in Kasalath rice variety (Gamuyao et al., 2012). This gene is responsible for early root growth in phosphorus-deficient soil and increases grain yield exponentially (Gamuyao et al., 2012). So, using a comparative genomics study, we have tried to locate and identify ortholog of *PSTOL1* gene in wheat just like it was done previously in *Sorghum bicolor* by (Hufnagel et al., 2014) and in *Zea mays* by (Azevedo et al., 2015) .

In our study, we used two wheat varieties, Pak-13 and Shafaq-06. Both varieties were grown under phosphorus-deficient and sufficient conditions, similar to the study (Wang et al., 2019). Shafaq-06 plants under phosphorus-deficient conditions showed reduced shoot dry weight, root dry weight, and total root length similar to (Horst et al., 1993). Shafaq-06 contained low phosphorus content in both shoots and roots. Also, following (Alam et al., 2001), our wheat plants showed low levels of chlorophyll under low phosphorus content, Shafaq-06 in our study exhibited lower levels of chlorophyll content under phosphorus-deficient conditions along with a lower number of tillers (Pandey et al., 2005). On the other hand, Pak-13 plants tried to survive and thrive in phosphorus-deficient conditions. Pak-13 plants showed increased root length, root dry weight, tiller count under phosphorus deficiency (Horst et al., 1993). Pak-13 also displayed more phosphorus content than Shafaq-06 plants under phosphorus stress, in both shoots and roots, and higher chlorophyll content. Based on these inferences, we conclude that Pak-13 is phosphorus efficient variety, while Shafaq-06 is non-efficient to phosphorus uptake.

This study identified 22 orthologs of *PSTOL1* in *Triticum aestivum L.* through BLASTP, conserved motifs, domains, and expression analysis. Previously, 6 orthologs were identified in *Sorghum bicolor* (Hufnagel et al., 2014), and 6 were identified in *Zea mays* (Azevedo et al., 2015). Similar to these previous studies, all 22 orthologs in our study contained conserved Ser/Thr kinase domain. Along with this conserved domain, these orthologs also included features similar to *OsPSTOL1* and *SbPSTOL1*. One was the presence of wall-associated kinases or WAKs domain, which links the cytoplasm and the pectin fraction of the cell wall and is also responsible for generating stress response (Kohorn and Kohorn, 2012; Kaur et al., 2013). WAKs are also found to cause root extension and elongation in barley (*Hordeum vulgare*).

Along with that the WAKs interact with other genes as a stress response for alteration of root development (Tripathi et al., 2021). According to (Hufnagel et al., 2014), the interaction of the cell wall and cell membrane may cause increased root surface area and phosphorus uptake during stress. Along with WAKs, some of the wheat orthologs also contained the GUB-WAK bind domain.

To validate and confirm that some genes show upregulation and some genes exhibit downregulation under phosphorus starvation stress (Wang et al., 2019), we selected 4 genes out of 22 orthologs based on the transcriptomic data obtained from the study of (Oono et al., 2013). Among these genes, 3 showed upregulation under phosphorus stress while 1 gene showed downregulation. Upon performing RT-PCR, 3 of our genes showed similar results while the fourth gene showed the contrary. In Pak-13, similar to transcriptomic data, the TraesCS3A02G018500 gene showed upregulation under phosphorus starvation. Shafaq-06 plants showed higher expression under stress than control but displayed very high relative expression under sufficient phosphorus. We assume that Shafaq-06 plants underwent more stress during the excess of phosphorus. The other two genes TraesCS5B02G391900 and TraesCS5D02G396800 also showed a similar result. Both of these genes were up-regulated in phosphorus-deficient conditions compared to control, but they all were also highly expressed in +P conditions for both varieties.

Conclusion

Pak-13 is identified to be more phosphorus efficient. It shows enhanced root growth and deeper root architecture with increased phosphorus uptake under phosphorus starvation. With these findings Pak-13 should be introduced into breeding programs for further development of new varieties with enhanced P-uptake efficiency. The three putative candidate genes for *PSTOL1,* identified in this study, will lay foundation for further exploration of these genes and their functions. Novel gene editing tools like CRISPR-Cas9, ZFNs and RNAi should be utilized to further validate the function of these genes. This study also improves our understanding of *Phosphorus Starvation Tolerance 1* (*PSTOL1*) gene in phosphorus uptake, root development and plant growth. Utilization and selection based on the *PSTOL1* gene will help us to improve the phosphorus use efficiency in wheat varieties.

REFERENCES

Ahmad, A., Ashfaq, M., Rasul, G., Wajid, S.A., Khaliq, T., Rasul, F., et al. (2015). "Impact of climate change on the rice–wheat cropping system of Pakistan," in *Handbook of Climate Change and Agroecosystems: The Agricultural Model Intercomparison and Improvement Project Integrated Crop and Economic Assessments, Part 2*.), 219-258.

Alam, S., Khanzada, B., Ali, M., Khan, M., and Ansari, R. (2001). Effect of different levels of zinc and phosphorus on growth and chlorophyll contents of wheat. *Pak. J. Agric. Agric. Eng. Vet. Sci.*

Alaux, M., Rogers, J., Letellier, T., Flores, R., Alfama, F., Pommier, C., et al. (2018). Linking the International Wheat Genome Sequencing Consortium bread wheat reference genome sequence to wheat genetic and phenomic data. *Genome biology* 19**,** 1-10.

Arnon, D.I. (1949). Copper Enzymes in Isolated Chloroplasts. Polyphenoloxidase in Beta Vulgaris. *Plant Physiol.* 24**,** 1-15. doi: 10.1104/pp.24.1.1.

Avni, R., Nave, M., Barad, O., Baruch, K., Twardziok, S.O., Gundlach, H., et al. (2017). Wild emmer genome architecture and diversity elucidate wheat evolution and domestication. *Science* 357**,** 93-97.

Azevedo, G.C., Cheavegatti-Gianotto, A., Negri, B.F., Hufnagel, B., C, E.S.L., Magalhaes, J.V., et al. (2015). Multiple interval QTL mapping and searching for PSTOL1 homologs associated with root morphology, biomass accumulation and phosphorus content in maize seedlings under low-P. *BMC Plant Biol.* 15**,** 172. doi: 10.1186/s12870-015-0561-y.

Bailey, T.L., Johnson, J., Grant, C.E., and Noble, W.S. (2015). The MEME Suite. *Nucleic Acids Res.* 43**,** W39-49. doi: 10.1093/nar/gkv416.

Baillo, E.H., Kimotho, R.N., Zhang, Z., and Xu, P. (2019). Transcription factors associated with abiotic and biotic stress tolerance and their potential for crops improvement. *Genes* 10**,** 771.

Bariah, I., Keidar-Friedman, D., and Kashkush, K. (2020). Identification and characterization of large-scale genomic rearrangements during wheat evolution. *PloS one* 15**,** e0231323.

Blake, V.C., Woodhouse, M.R., Lazo, G.R., Odell, S.G., Wight, C.P., Tinker, N.A., et al. (2019). GrainGenes: centralized small grain resources and digital platform for geneticists and breeders. *Database (Oxford)* 2019. doi: 10.1093/database/baz065.

Borrill, P., Ramirez-Gonzalez, R., and Uauy, C. (2016). expVIP: a Customizable RNA-seq Data Analysis and Visualization Platform. *Plant Physiol.* 170**,** 2172-2186. doi: 10.1104/pp.15.01667.

Carstensen, A., Herdean, A., Schmidt, S.B., Sharma, A., Spetea, C., Pribil, M., et al. (2018). The impacts of phosphorus deficiency on the photosynthetic electron transport chain. *Plant physiology* 177**,** 271-284.

Chaudhary, M.I., Adu-Gyamfi, J.J., Saneoka, H., Nguyen, N.T., Suwa, R., Kanai, S., et al. (2008). The effect of phosphorus deficiency on nutrient uptake, nitrogen fixation and photosynthetic rate in mashbean, mungbean and soybean. *Acta Physiol. Plantarum* 30**,** 537-544.

Chen, C., Chen, H., He, Y., and Xia, R. (2018). TBtools, a toolkit for biologists integrating various biological data handling tools with a user-friendly interface. *BioRxiv* 289660.

Chen, S., Zhao, H., Ding, G., and Xu, F. (2015). Genotypic differences in antioxidant response to phosphorus deficiency in Brassica napus. *Plant Soil* 391**,** 19-32.

El Baidouri, M., Murat, F., Veyssiere, M., Molinier, M., Flores, R., Burlot, L., et al. (2017). Reconciling the evolutionary origin of bread wheat (Triticum aestivum). *New Phytologist* 213**,** 1477-1486.

Frydenvang, J., van Maarschalkerweerd, M., Carstensen, A., Mundus, S., Schmidt, S.B., Pedas, P.R., et al. (2015). Sensitive detection of phosphorus deficiency in plants using chlorophyll a fluorescence. *Plant Physiol.* 169**,** 353-361.

Gamuyao, R., Chin, J.H., Pariasca-Tanaka, J., Pesaresi, P., Catausan, S., Dalid, C., et al. (2012). The protein kinase Pstol1 from traditional rice confers tolerance of phosphorus deficiency. *Nature* 488**,** 535-539. doi: 10.1038/nature11346.

Gemenet, D.C., Leiser, W.L., Beggi, F., Herrmann, L.H., Vadez, V., Rattunde, H.F., et al. (2016). Overcoming Phosphorus Deficiency in West African Pearl Millet and Sorghum Production Systems: Promising Options for Crop Improvement. *Front. Plant Sci.* 7**,** 1389. doi: 10.3389/fpls.2016.01389.

Guo, Y., Kong, F.M., Xu, Y.F., Zhao, Y., Liang, X., Wang, Y.Y., et al. (2012). QTL mapping for seedling traits in wheat grown under varying concentrations of N, P and K nutrients. *Theor. Appl. Genet.* 124**,** 851-865. doi: 10.1007/s00122-011-1749-7.

Gupta, P.K., Balyan, H.S., Sharma, S., and Kumar, R. (2020). Genetics of yield, abiotic stress tolerance and biofortification in wheat (Triticum aestivum L.). *Theoretical and Applied Genetics* 133**,** 1569-1602.

Haider, S.A., Naqvi, S.R., Akram, T., Umar, G.A., Shahzad, A., Sial, M.R., et al. (2019). LSTM neural network based forecasting model for wheat production in Pakistan. *Agronomy* 9**,** 72.

Hammond, J.P., Broadley, M.R., and White, P.J. (2004). Genetic responses to phosphorus deficiency. *Annals of botany* 94**,** 323-332.

Horst, W., Abdou, M., and Wiesler, F. (1993). Genotypic differences in phosphorus efficiency of wheat. *Plant Soil* 155**,** 293-296.

Hu, B., Jin, J., Guo, A.Y., Zhang, H., Luo, J., and Gao, G. (2015). GSDS 2.0: an upgraded gene feature visualization server. *Bioinformatics* 31**,** 1296-1297. doi: 10.1093/bioinformatics/btu817.

Hufnagel, B., de Sousa, S.M., Assis, L., Guimaraes, C.T., Leiser, W., Azevedo, G.C., et al. (2014). Duplicate and conquer: multiple homologs of PHOSPHORUS-STARVATION TOLERANCE1 enhance phosphorus acquisition and sorghum performance on low-phosphorus soils. *Plant. Physiol.* 166**,** 659-677. doi: 10.1104/pp.114.243949.

Kaur, R., Singh, K., and Singh, J. (2013). A root-specific wall-associated kinase gene, HvWAK1, regulates root growth and is highly divergent in barley and other cereals. *Funct. integr. genomics* 13**,** 167-177.

Khaliq, T., Gaydon, D.S., Cheema, M., and Gull, U. (2019). Analyzing crop yield gaps and their causes using cropping systems modelling–A case study of the Punjab rice-wheat system, Pakistan. *Field Crops Research* 232**,** 119-130.

Kochian, L.V. (2012). Rooting for more phosphorus. *Nature* 488**,** 466-467.

Kohorn, B.D., and Kohorn, S.L. (2012). The cell wall-associated kinases, WAKs, as pectin receptors. *Front. plant sci.* 3**,** 88.

Kono, T.J.Y., Lei, L., Shih, C.H., Hoffman, P.J., Morrell, P.L., and Fay, J.C. (2018). Comparative Genomics Approaches Accurately Predict Deleterious Variants in Plants. *G3 (Bethesda)* 8**,** 3321-3329. doi: 10.1534/g3.118.200563.

Kumar, S., Tamura, K., and Nei, M. (1994). MEGA: Molecular Evolutionary Genetics Analysis software for microcomputers. *Bioinformatics* 10**,** 189-191. doi: 10.1093/bioinformatics/10.2.189.

Kuo, H.F., and Chiou, T.J. (2011). The role of microRNAs in phosphorus deficiency signaling. *Plant Physiol.* 156**,** 1016-1024. doi: 10.1104/pp.111.175265.

Lan, P., Li, W., and Schmidt, W. (2018). 'Omics' approaches towards understanding plant phosphorus acquisition and use. *Annu. Plant Rev.* 65-97.

Lehti-Shiu, M.D., Zou, C., Hanada, K., and Shiu, S.H. (2009). Evolutionary history and stress regulation of plant receptor-like kinase/pelle genes. *Plant Physiol.* 150**,** 12-26. doi: 10.1104/pp.108.134353.

Leiser, W.L., Rattunde, H.F.W., Piepho, H.P., Weltzien, E., Diallo, A., Melchinger, A.E., et al. (2012). Selection strategy for sorghum targeting phosphorus-limited environments in West Africa: Analysis of multi-environment experiments. *Crop Science* 52**,** 2517-2527.

Lescot, M., Dehais, P., Thijs, G., Marchal, K., Moreau, Y., Van de Peer, Y., et al. (2002). PlantCARE, a database of plant cis-acting regulatory elements and a portal to tools for in silico analysis of promoter sequences. *Nucleic Acids Res.* 30**,** 325-327. doi: 10.1093/nar/30.1.325.

Letunic, I., and Bork, P. (2018). 20 years of the SMART protein domain annotation resource. *Nucleic Acids Res.* 46**,** D493-D496. doi: 10.1093/nar/gkx922.

Letunic, I., and Bork, P. (2021). Interactive Tree Of Life (iTOL) v5: an online tool for phylogenetic tree display and annotation. *Nucleic Acids Res.* 49**,** W293-W296. doi: 10.1093/nar/gkab301.

Lichtenthaler, H.K. (1987). [34] Chlorophylls and carotenoids: pigments of photosynthetic biomembranes. *Meth. enzymol.* 148**,** 350-382.

Lynch, M., O'Hely, M., Walsh, B., and Force, A. (2001). The probability of preservation of a newly arisen gene duplicate. *Genetics* 159**,** 1789-1804. doi: 10.1093/genetics/159.4.1789.

Malhotra, H., Sharma, S., and Pandey, R. (2018). "Phosphorus nutrition: plant growth in response to deficiency and excess," in *Plant nutrients and abiotic stress tolerance*. Springer), 171-190.

McDonald, G., Bovill, W., Taylor, J., and Wheeler, R. (2015). Responses to phosphorus among wheat genotypes. *Crop Pasture Sci.* 66**,** 430-444.

Moriondo, M., Maselli, F., and Bindi, M. (2007). A simple model of regional wheat yield based on NDVI data. *European Journal of Agronomy* 26**,** 266-274.

Oono, Y., Kobayashi, F., Kawahara, Y., Yazawa, T., Handa, H., Itoh, T., et al. (2013). Characterisation of the wheat (Triticum aestivum L.) transcriptome by de novo assembly for the discovery of phosphate starvation-responsive genes: gene expression in Pi-stressed wheat. *BMC Genomics* 14**,** 77. doi: 10.1186/1471-2164-14-77.

Pandey, R., Singh, B., and Nair, T. (2005). Phosphorus use efficiency of wheat, rye and triticale under deficient and sufficient levels of phosphorus. *Indian J. Plant Physiol.* 10**,** 292.

Pudake, R.N., Mehta, C.M., Mohanta, T.K., Sharma, S., Varma, A., and Sharma, A.K. (2017). Expression of four phosphate transporter genes from Finger millet (Eleusine coracana L.) in response to mycorrhizal colonization and Pi stress. *3 Biotech* 7**,** 17.

Raza, A., Mehmood, S.S., Tabassum, J., and Batool, R. (2019). "Targeting plant hormones to develop abiotic stress resistance in wheat," in *Wheat production in changing environments*. Springer), 557-577.

Ren, Y., Qian, Y., Xu, Y., Zou, C., Liu, D., Zhao, X., et al. (2017). Characterization of QTLs for Root Traits of Wheat Grown under Different Nitrogen and Phosphorus Supply Levels. *Front. Plant Sci.* 8**,** 2096. doi: 10.3389/fpls.2017.02096.

Salim, N., and Raza, A. (2020). Nutrient use efficiency (NUE) for sustainable wheat production: a review. *Journal of Plant Nutrition* 43**,** 297-315.

Sattari, S.Z., Bouwman, A.F., Giller, K.E., and van Ittersum, M.K. (2012). Residual soil phosphorus as the missing piece in the global phosphorus crisis puzzle. *Proceedings of the National Academy of Sciences* 109**,** 6348-6353.

Seethepalli, A., Guo, H., Liu, X., Griffiths, M., Almtarfi, H., Li, Z., et al. (2020). RhizoVision Crown: An Integrated Hardware and Software Platform for Root

Crown Phenotyping. *Plant Phenomics* 2020**,** 3074916. doi: 10.34133/2020/3074916.

Shar, G., Kazi, T., Jakhrani, M., and Sahito, S. (2002). Determination of Iron, Zinc and Manganese in Nine Varieties of Wheat (Triticum aestivum L.) and Wheat Flour by using Atomic Absorption Spectrophotometer. *Asian J. Plant Sci.*

Sharma, I., Tyagi, B., Singh, G., Venkatesh, K., and Gupta, O. (2015). Enhancing wheat production-A global perspective. *Indian Journal of Agricultural Sciences* 85**,** 3-13.

Shewry, P.R., and Hey, S.J. (2015). The contribution of wheat to human diet and health. *Food and energy security* 4**,** 178-202.

Shi, R., Li, H., Tong, Y., Jing, R., Zhang, F., and Zou, C. (2008). Identification of quantitative trait locus of zinc and phosphorus density in wheat (Triticum aestivum L.) grain. *Plant Soil* 306**,** 95-104.

Simms, D., Cizdziel, P.E., and Chomczynski, P. (1993). TRIzol: A new reagent for optimal single-step isolation of RNA. *Focus* 15**,** 532-535.

Singla, J., Krattinger, S., Wrigley, C., Faubion, J., Corke, H., and Seetharaman, K. (2016). Biotic stress resistance genes in wheat.

Song, X., Liu, Z., Wan, H., Chen, W., Zhou, R., and Duan, W. (2021). Editorial: Comparative Genomics and Functional Genomics Analyses in Plants. *Front. Genet.* 12**,** 687966. doi: 10.3389/fgene.2021.687966.

Soumya, P.R., Sharma, S., Meena, M.K., and Pandey, R. (2021). Response of diverse bread wheat genotypes in terms of root architectural traits at seedling stage in response to low phosphorus stress. *Plant Physiol. Rep.* 26**,** 152-161.

Stangoulis, J. (2019). Variation in root system architecture and morphology of two wheat genotypes is a predictor of their tolerance to phosphorus deficiency. *Acta Physiologiae Plantarum* 41**,** 1-13.

Sulieman, S., and Tran, L.-S.P. (2015). Phosphorus homeostasis in legume nodules as an adaptive strategy to phosphorus deficiency. *Plant Science* 239**,** 36-43.

Tadesse, W., Halila, H., Jamal, M., El-Hanafi, S., Assefa, S., Oweis, T., et al. (2017). Role of sustainable wheat production to ensure food security in the CWANA region. *Journal of Experimental Biology and Agricultural Sciences* 5.

Thompson, J.D., Gibson, T.J., and Higgins, D.G. (2003). Multiple sequence alignment using ClustalW and ClustalX. *Curr. Protoc. Bioinformatics* 2.3. 1-2.3. 22.

Tripathi, R.K., Aguirre, J.A., and Singh, J. (2021). Genome-wide analysis of wall associated kinase (WAK) gene family in barley. *Genomics* 113**,** 523-530. doi: 10.1016/j.ygeno.2020.09.045.

Tyagi, S., Shumayla, Verma, P.C., Singh, K., and Upadhyay, S.K. (2020). Molecular characterization of ascorbate peroxidase (APX) and APX-related (APX-R) genes in Triticum aestivum L. *Genomics* 112**,** 4208-4223. doi: 10.1016/j.ygeno.2020.07.023.

UYGUR, V., and Mustafa, Ş. (2018). The effect of phosphorus application on nutrient uptake and translocation in wheat cultivars. *Intern. J. Agric. Forest. Life Sci.* 2**,** 171-179.

Vejchasarn, P., Lynch, J.P., and Brown, K.M. (2016). Genetic Variability in Phosphorus Responses of Rice Root Phenotypes. *Rice (N Y)* 9**,** 29. doi: 10.1186/s12284-016-0102-9.

Veneklaas, E.J., Lambers, H., Bragg, J., Finnegan, P.M., Lovelock, C.E., Plaxton, W.C., et al. (2012). Opportunities for improving phosphorus-use efficiency in crop plants. *New Phytol.* 195**,** 306-320. doi: 10.1111/j.1469-8137.2012.04190.x.

Vigueira, C.C., Small, L.L., and Olsen, K.M. (2016). Long-term balancing selection at the Phosphorus Starvation Tolerance 1 (PSTOL1) locus in wild, domesticated and weedy rice (Oryza). *BMC Plant Biol.* 16**,** 1-10.

Voorrips, R.E. (2002). MapChart: software for the graphical presentation of linkage maps and QTLs. *J. Hered* 93**,** 77-78. doi: 10.1093/jhered/93.1.77.

Wang, D., Zhang, Y., Zhang, Z., Zhu, J., and Yu, J. (2010). KaKs_Calculator 2.0: a toolkit incorporating gamma-series methods and sliding window strategies. *Genomics Proteomics Bioinformatics* 8**,** 77-80. doi: 10.1016/S1672-0229(10)60008-3.

Wang, J., Qin, Q., Pan, J., Sun, L., Sun, Y., Xue, Y., et al. (2019). Transcriptome analysis in roots and leaves of wheat seedlings in response to low-phosphorus stress. *Sci. Rep.* 9**,** 19802. doi: 10.1038/s41598-019-56451-6.

Wang, Y., Tang, H., Debarry, J.D., Tan, X., Li, J., Wang, X., et al. (2012). MCScanX: a toolkit for detection and evolutionary analysis of gene synteny and collinearity. *Nucleic Acids Res.* 40**,** e49. doi: 10.1093/nar/gkr1293.

Yang, M., Wang, C., Hassan, M.A., Li, F., Xia, X., Shi, S., et al. (2021). QTL mapping of root traits in wheat under different phosphorus levels using hydroponic culture. *BMC genomics* 22**,** 1-12.

Yang, X., Liu, Y., Wu, F., Jiang, X., Lin, Y., Wang, Z., et al. (2018). Quantitative trait loci analysis of root traits under phosphorus deficiency at the seedling stage in wheat. *Genome* 61**,** 209-215.

Ye, J., Coulouris, G., Zaretskaya, I., Cutcutache, I., Rozen, S., and Madden, T.L. (2012). Primer-BLAST: a tool to design target-specific primers for polymerase chain reaction. *BMC Bioinformatics* 13**,** 134. doi: 10.1186/1471-2105-13-134.

Yi-Qin, H., Wen-di, H., Lei, Y., Yi-Ting, L., Chen, L., Yong-Xing, Z., et al. (2020). Genome-wide analysis of ethylene-insensitive3 (EIN3/EIL) in Triticum aestivum. *Crop Sci.* 60**,** 2019-2037.

Yuan, Y., Gao, M., Zhang, M., Zheng, H., Zhou, X., Guo, Y., et al. (2017). QTL mapping for phosphorus efficiency and morphological traits at seedling and maturity stages in wheat. *Front. Plant Sci.* 8**,** 614.

Yuan, Y., Zhang, M., Zheng, H., Kong, F., Guo, Y., Zhao, Y., et al. (2020). Detection of QTL for phosphorus efficiency and biomass traits at the seedling stage in wheat. *Cereal Research Communications* 48**,** 517-524.

Zambrosi, F.C.B., Ribeiro, R.V., Marchiori, P.E.R., Cantarella, H., and Landell, M.G.A. (2015). Sugarcane performance under phosphorus deficiency: physiological responses and genotypic variation. *Plant and soil* 386**,** 273-283.

Zhang, T., Wen, X.-P., and Ding, G.-J. (2017). Ectomycorrhizal symbiosis enhances tolerance to low phosphorous through expression of phosphate transporter genes in masson pine (Pinus massoniana). *Acta Physiologiae Plantarum* 39**,** 101.

Zhang, Z., Xiao, J., Wu, J., Zhang, H., Liu, G., Wang, X., et al. (2012). ParaAT: a parallel tool for constructing multiple protein-coding DNA alignments. *Biochem Biophys Res Commun* 419**,** 779-781. doi: 10.1016/j.bbrc.2012.02.101.

Appendix - I

ANOVA for Tiller Count

Source	DF	MS	P-Value
Genotypes	1	0.05556	0.7787
Treatment	2	1.16667	0.2230
Genotypes*Treatment	2	0.05556	0.9207

LSD for Genotype

Treatment	Homogeneous Groups
1	A
2	A

LSD for Treatment

Treatment	Homogeneous Groups
2	A
3	A
1	A

LSD for Treatment*Genotype

Genotypes	Treatment	Homogeneous Groups
1	2	A
2	2	A
1	1	A
1	3	A
2	3	A
2	2	A

Appendix - II

ANOVA for Shoot Length

Source	DF	MS	P-Value
Genotypes	1	0.0200	0.9675
Treatment	2	25.4606	0.1591
Genotypes*Treatment	2	16.0317	0.2913

LSD for Genotype

Treatment	Homogeneous Groups
1	A
2	A

LSD for Treatment

Treatment	Homogeneous Groups
2	A
3	A
1	A

LSD for Treatment*Genotype

Genotypes	Treatment	Homogeneous Groups
2	2	A
1	2	A
1	3	A
2	1	A
1	1	A
2	3	A

Appendix - III

ANOVA for Fresh Shoot Weight

Source	DF	MS	P-Value
Genotypes	1	0.05163	0.8066
Treatment	2	2.54119	0.0891
Genotypes*Treatment	2	0.02233	0.9731

LSD for Genotype

Treatment	Homogeneous Groups
1	A
2	A

LSD for treatment

Treatment	Homogeneous Groups
2	A
1	A
3	A

LSD for Treatment*Genotype

Genotypes	Treatment	Homogeneous Groups
1	2	A
2	2	A
1	1	A
2	1	A
1	**3**	**A**
2	3	A

Appendix - IV

ANOVA for Dry Shoot Weight

Source	DF	MS	P-Value
Genotypes	1	0.00448	0.6220
Treatment	2	0.03636	0.1732
Genotypes*Treatment	2	0.00064	0.9637

LSD for Genotype

Treatment	Homogeneous Groups
2	A
1	A

LSD for Treatment

Treatment	Homogeneous Groups
2	A
3	A
1	A

LSD for Treatment*Genotype

Genotypes	Treatment	Homogeneous Groups
1	2	A
2	2	A
1	1	A
2	1	A
1	3	A
2	3	A

Appendix - V

ANOVA for Fresh Root Weight

Source	DF	MS	P-Value
Genotypes	1	1.12400	0.0230
Treatment	2	0.44579	0.1046
Genotypes*Treatment	2	0.01589	0.9042

LSD for Genotype

Treatment	Homogeneous Groups
2	A
1	B

LSD for Treatment

Treatment	Homogeneous Groups
2	A
3	A
1	A

LSD for Treatment*Genotype

Genotypes	Treatment	Homogeneous Groups
2	2	A
2	3	AB
1	2	AB
2	1	AB
1	3	B
1	1	B

Appendix - VI

ANOVA for Dry Root Weight

Source	DF	MS	P-Value
Genotypes	1	0.01307	0.0396
Treatment	2	0.00506	0.1654
Genotypes*Treatment	2	0.00043	0.8363

LSD for Genotype

Treatment	Homogeneous Groups
2	A
1	B

LSD for Treatment

Treatment	Homogeneous Groups
2	A
3	A
1	A

LSD for Treatment*Genotype

Genotypes	Treatment	Homogeneous Groups
2	2	A
2	1	AB
1	2	AB

2	3	AB
1	3	B
1	1	B

Appendix - VII

ANOVA for Chlorophyll Content

Source	DF	MS	P-Value
Genotypes	1	33928	0.4404
Treatment	2	1426658	0.0017
Genotypes*Treatment	2	124734	0.1699

LSD for Genotype

Treatment	Homogeneous Groups
2	A
1	A

LSD for Treatment

Treatment	Homogeneous Groups
1	A
2	A
3	B

LSD for Treatment*Genotype

Genotypes	Treatment	Homogeneous Groups
1	1	A
2	2	A
2	1	A
1	2	A
1	3	B
2	3	B

Appendix - VIII

ANOVA for Shoot Phosphorus Content

Source	DF	MS	P-Value
Genotypes	2	0.18596	0.0185
Treatment	1	0.00714	0.5918
Genotypes*Treatment	2	0.01865	0.4778

LSD for Genotype

Treatment	Homogeneous Groups
2	A
1	A

LSD for Treatment

Treatment	Homogeneous Groups
2	A
3	B
1	B

LSD for Treatment*Genotype

Genotypes	Treatment	Homogeneous Groups
2	2	A
2	1	AB
3	1	ABC
3	2	BC
1	2	C
1	1	C

Appendix - IX

ANOVA for Root Phosphorus Content

Source	DF	MS	P-Value
Genotypes	1	0.00013	0.5405
Treatment	2	0.00228	0.0197
Genotypes*Treatment	2	0.00154	0.0467

LSD for Genotype

Treatment	Homogeneous Groups
1	A
2	A

LSD for Treatment

Treatment	Homogeneous Groups
2	A
1	B
3	B

LSD for Treatment*Genotype

Genotypes	Treatment	Homogeneous Groups
1	2	A
2	2	A
1	1	A
2	3	AB
2	1	B
1	3	B

Appendix - X

ANOVA for Root Length (RhizoVision Explorer)

Source	DF	MS	P-Value
Genotypes	1	152223	0.0375
Treatment	2	9447	0.7085
Genotypes*Treatment	2	799798	0.0001

LSD for Genotype

Treatment	Homogeneous Groups
2	A
1	B

LSD for Treatment

Treatment	Homogeneous Groups
3	A
1	A
2	A

LSD for Treatment*Genotype

Genotypes	Treatment	Homogeneous Groups
2	3	A
1	2	A
2	1	A
1	1	B
1	3	B
2	2	B

Appendix - XI

ANOVA for Root Diameter (RhizoVision Explorer)

Source	DF	MS	P-Value
Genotypes	2	1.12692	0.0237
Treatment	1	2.79716	0.0040
Genotypes*Treatment	2	0.45452	0.1565

LSD for Genotype

Treatment	Homogeneous Groups
1	A
2	B

LSD for Treatment

Treatment	Homogeneous Groups
1	A
2	B
3	B

LSD for Treatment*Genotype

Genotypes	Treatment	Homogeneous Groups
1	1	A
2	1	B
3	1	B
1	2	B
2	2	B
3	2	B

Appendix - XII

ANOVA for Root Volume (RhizoVision Explorer)

Source	DF	MS	P-Value
Genotypes	2	1.667E+07	0.0061
Treatment	1	1.812E+07	0.0111
Genotypes*Treatment	2	5.704E+07	0.0001

LSD for Genotype

Treatment	Homogeneous Groups
1	A
2	B

LSD for Treatment

Treatment	Homogeneous Groups
1	A
3	A
2	B

LSD for Treatment*Genotype

Genotypes	Treatment	Homogeneous Groups
1	1	A
3	2	B
2	1	C
3	1	CD
1	2	CD
2	2	D

Appendix - XIII

ANOVA for Root Surface Area (RhizoVision Explorer)

Source	DF	MS	P-Value
Genotypes	2	5767349	0.2842
Treatment	1	6549701	0.2312
Genotypes*Treatment	2	5.403E+07	0.0015

LSD for Genotype

Treatment	Homogeneous Groups
1	A
2	A

LSD for Treatment

Treatment	Homogeneous Groups
1	A
3	A
2	A

LSD for Treatment*Genotype

Genotypes	Treatment	Homogeneous Groups
1	1	A
3	2	A
2	1	AB
1	2	BC
2	2	BC
3	1	C

Molecular Characterization of Phosphorous Starvation Tolerance 1 Gene

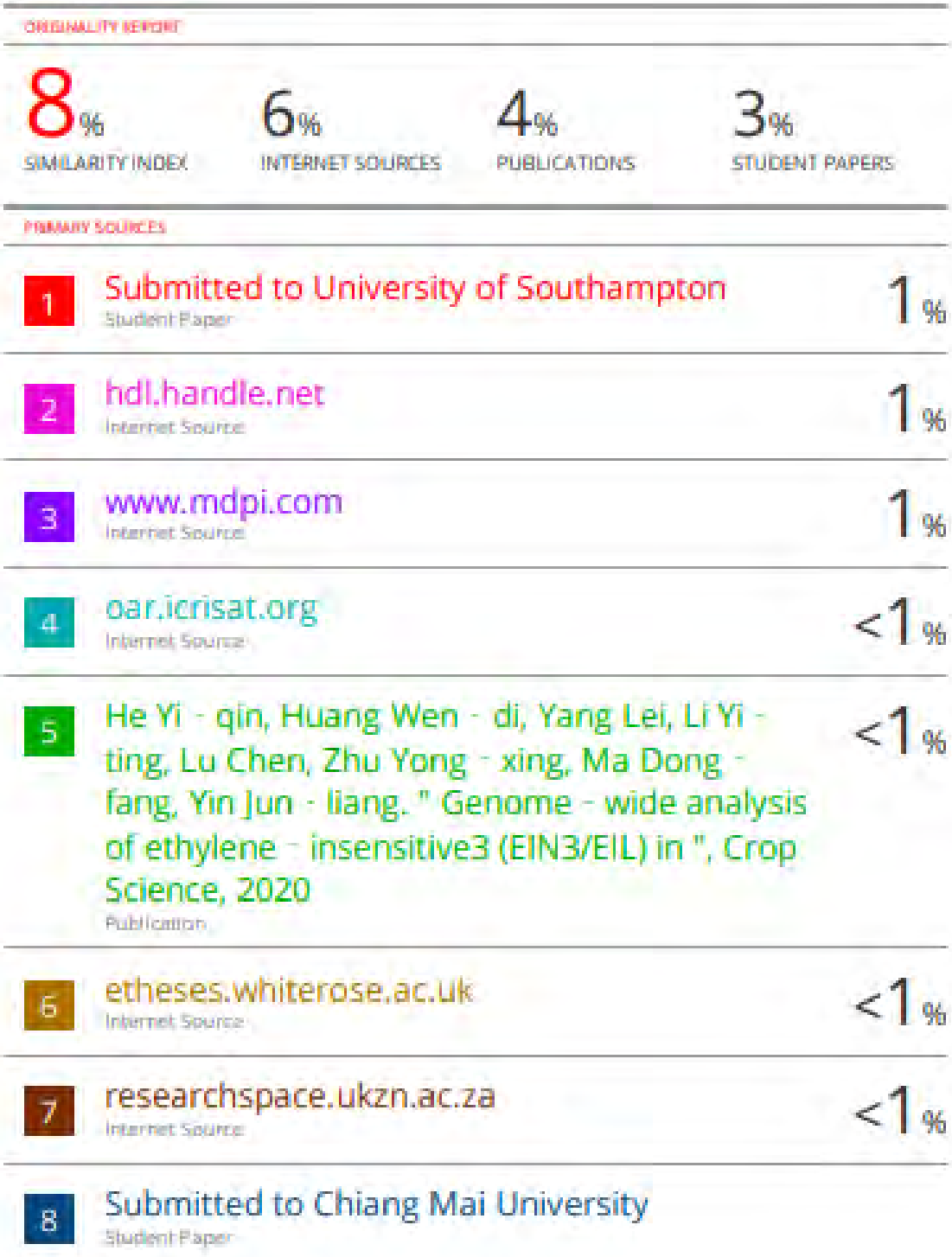

Dated: _____ Supervisor's Signature